Supporting Information

Selective Alkene Insertion into Inert Hydrogen-Metal Bond Catalyzed by Mono(phosphorus ligand)palladium(0) Complexes

Nobuyuki Komine,* Ryo Ito, Hiromi Suda, Masafumi Hirano, and Sanshiro Komiya

Department of Applied Chemistry, Graduate School of Engineering, Tokyo University of Agriculture and Technology, 2-24-16, Nakacho, Koganei, Tokyo 184-8588.

1. NMR data

Table S1. The spectram data of Pd(η^2,η^2-diallyl ether)(PR_3) (R = Et (1-Et), Bn (1-Bn), OEt (1-OEt), O^{i}Pr (1-O^{i}Pr), OXyl (1-OXyl)).

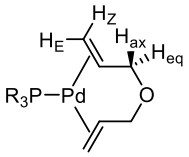

complex	δ(H)						δ(P)
	=CH–	H_Z	H_E	H_{eq}	H_{ax}	PR_3	
1-Et brown oil	3.97 (ddddd, J_{HH} = 2.9, 8.6, 11, 13Hz, J_{PH} = 4.2Hz)	2.64 (dd, J_{HH} = 13Hz, J_{PH} = 5.2Hz)	2.98 (dd, J_{HH} = 8.6Hz, J_{PH} = 5.2Hz)	4.79 (ddd, J_{HH} = 2.9, 13Hz, J_{PH} = 6.3Hz)	2.41 (dd, J_{HH} = 11, 13Hz)	0.84(dt, J_{HH} = 7.5Hz, J_{PH} = 15Hz, 9H, Me) 1.35(dq, J_{HH} = 7.5Hz, J_{PH} = 7.5Hz, 6H, PCH_2)	18.9
1-Bn yellow powder	4.01 (m)	2.36 (dd, J_{HH} = 11Hz, J_{PH} = 9.2Hz)	2.72 (dd, J_{HH} = 8.7Hz, J_{PH} = 5.0Hz)	4.72 (ddd, J_{HH} = 2.8, 11Hz, J_{PH} = 7.8Hz)	2.32 (dd, J_{HH} = 6.0, 13Hz)	2.90(d, J = 6.0Hz, 6H, PCH_2) 7.0(m, 15H, Ph)	18.2
1-OEt brown oil	3.97 (m)	2.98 (dd, J_{HH} = 14Hz, J_{PH} = 6.0Hz)	3.33 (dd, J_{HH} =8.6Hz, J_{PH} = 6.0Hz)	4.68 (dd, J_{HH} = 10Hz, J_{PH} = 10Hz)	2.41 (dd, J_{HH} = 11, 13Hz)	1.10(t, J_{HH} = 7.1Hz, 9H, Me) 3.86(dq, J_{HH} = 6.8Hz, J_{PH} = 6.8Hz, 6H, $POCH_2$)	160.4
1-OiPr brown oil	3.98 (ddddd, J_{HH} = 2.9, 8.6, 11, 13Hz, J_{PH} = 6.0Hz)	2.99 (dd, J_{HH} = 13Hz, J_{PH} = 5.7Hz)	3.32 (dd, J_{HH} = 8.6Hz, J_{PH} = 6.3Hz)	4.68 (ddd, J_{HH} = 2.9, 13Hz, J_{PH} = 9.2Hz)	2.41 (dd, J_{HH} = 11, 13Hz)	1.18(d, J_{HH} = 5.7Hz, 18H, Me) 4.58(dsept, J_{HH} = 6.3Hz, J_{PH} = 9.8Hz, 3H, POCH)	158.4
1-OXyl pale yellow crystals	3.90 (ddddd, J_{HH} = 2.3, 8.7, 12, 14Hz, J_{PH} = 6.0Hz)	2.56 (dd, J_{HH} = 14Hz, J_{PH} = 6.5Hz)	3.04 (dd, J_{HH} = 8.7Hz. J_{PH} = 6.5Hz)	4.45 (ddd, J_{HH} = 2.3, 12Hz, J_{PH} = 12Hz)	1.92 (dd, J_{HH} = 12, 12Hz)	2.32(s, 18H, Me) 6.80(s, 9H, Ph)	157.7
free diallyl ether	5.82(ddt, J = 11, 17, 5.0Hz)	5.22 (d, J = 17Hz)	5.02 (d, J = 11Hz)	3.78 (J = 1.4, 5.0Hz)			

^{1}H NMR spectrum assignment of W[CH(CO$_2$Me)(CH$_2$CO$_2$Me)]Cp(CO)$_3$

All three protons in α- and β-positions of WCp(CO)$_3$ in W[CH(CO$_2$Me)(CH$_2$CO$_2$Me)]Cp(CO)$_3$ and W[CD(CO$_2$Me)(CH$_2$CO$_2$Me)]Cp(CO)$_3$ were assigned with estimeted *J* values by Karplus equation as Chem Draw stucture in Figure S1.

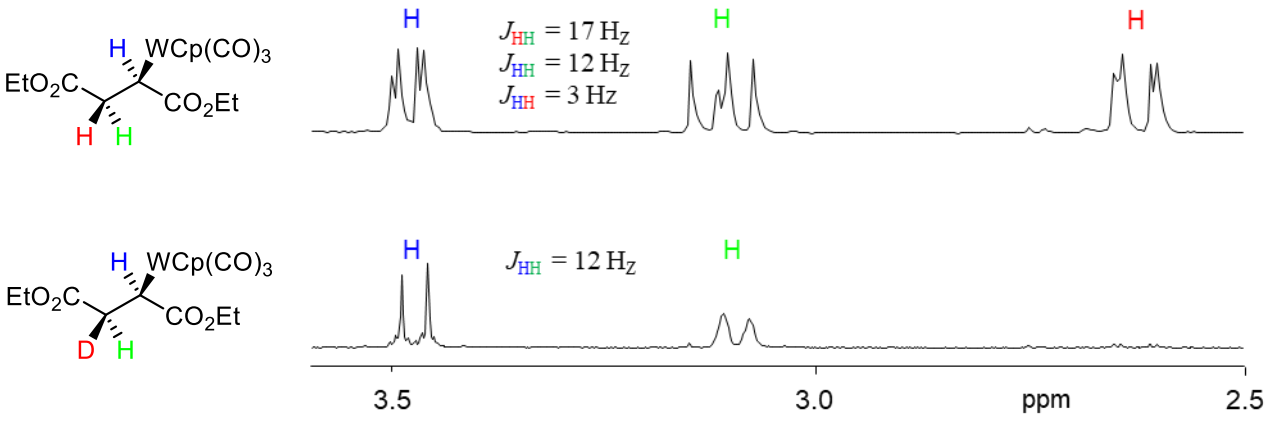

Figure S1. ^{1}H NMR spectra of W[CH(or D)(CO$_2$Me)(CH$_2$CO$_2$Me)]Cp(CO)$_3$.

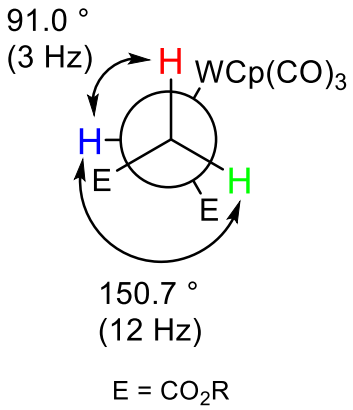

Figure S2. Most-stable conformer of W[CH(CO$_2$Me)(CH$_2$CO$_2$Me)]Cp(CO)$_3$ by DFT calculations. Estimeted *J* values by Karplus equation are indicated in parentheses

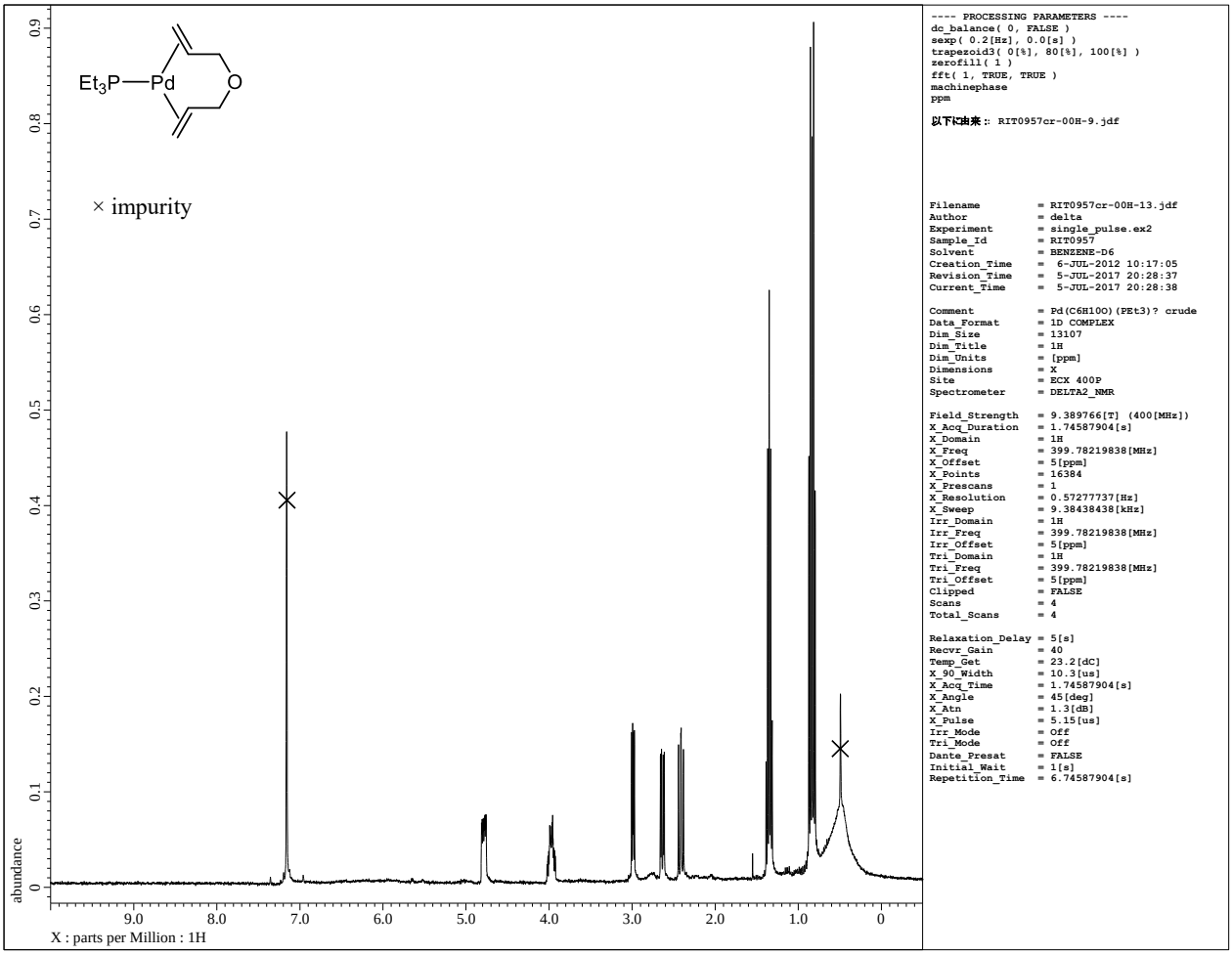

Figure S3. ^{1}H NMR spectra of Pd(η^2,η^2-diallyl ether)(PEt_3) (**1-Et**) (400 MHz, C_6D_6, 23 °C)

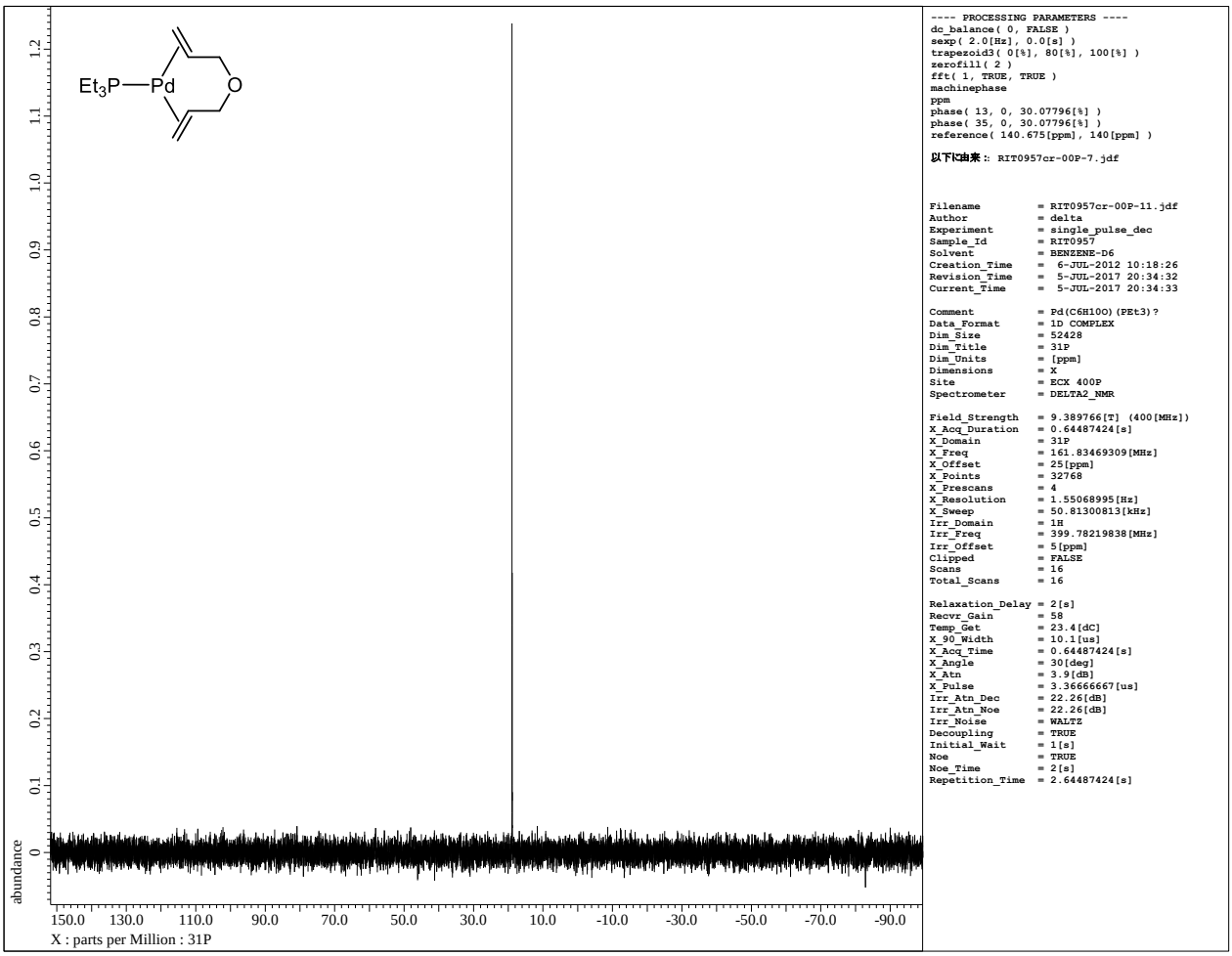

Figure S4. ^{31}P{^{1}H} NMR spectra of Pd(η^2,η^2-diallyl ether)(PEt_3) (**1-Et**) (162 MHz, C_6D_6, 23 °C)

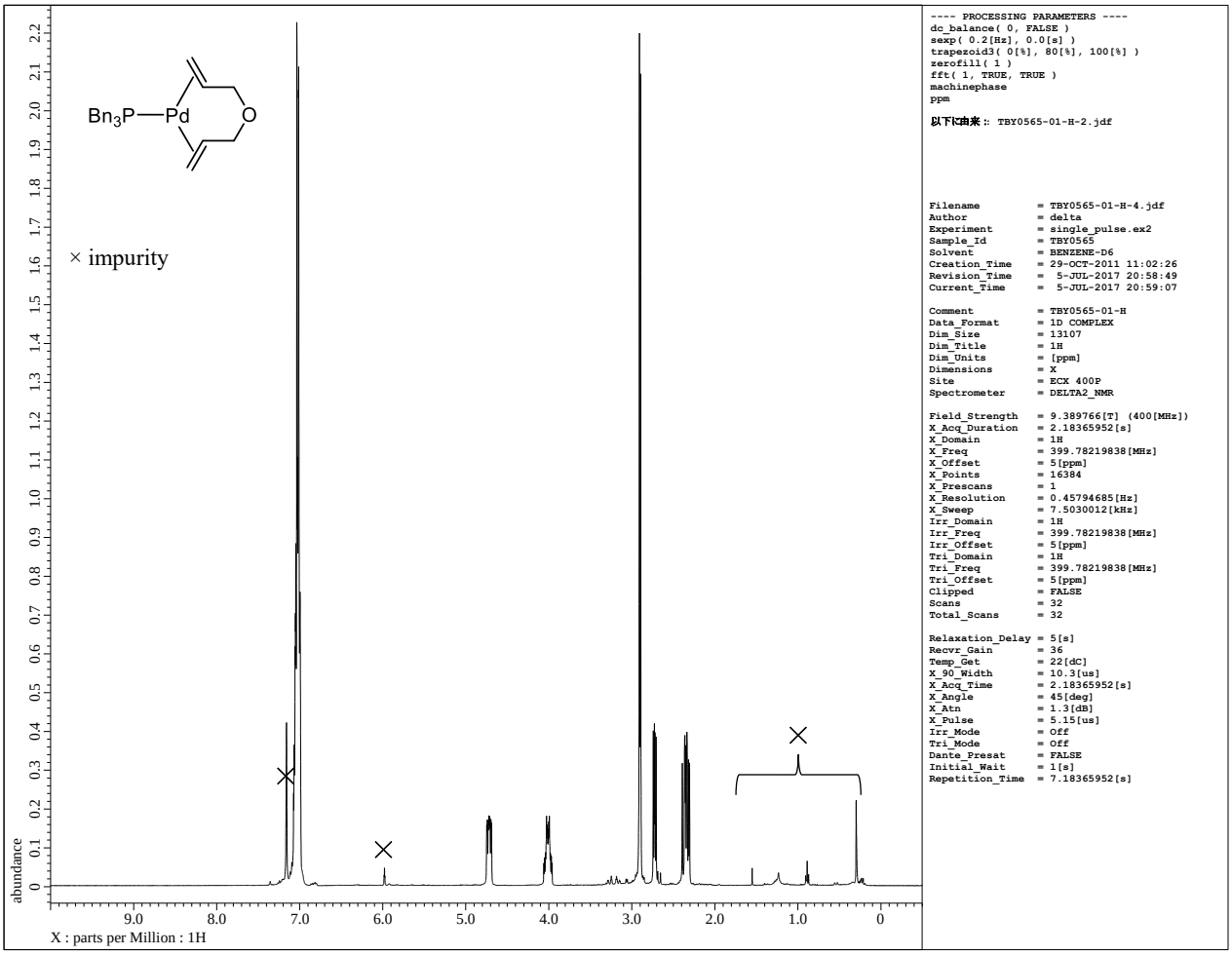

Figure S5. ^{1}H NMR spectra of Pd(η^2,η^2-diallyl ether)(PBn_3) (**1-Bn**) (400 MHz, C_6D_6, 22 °C)

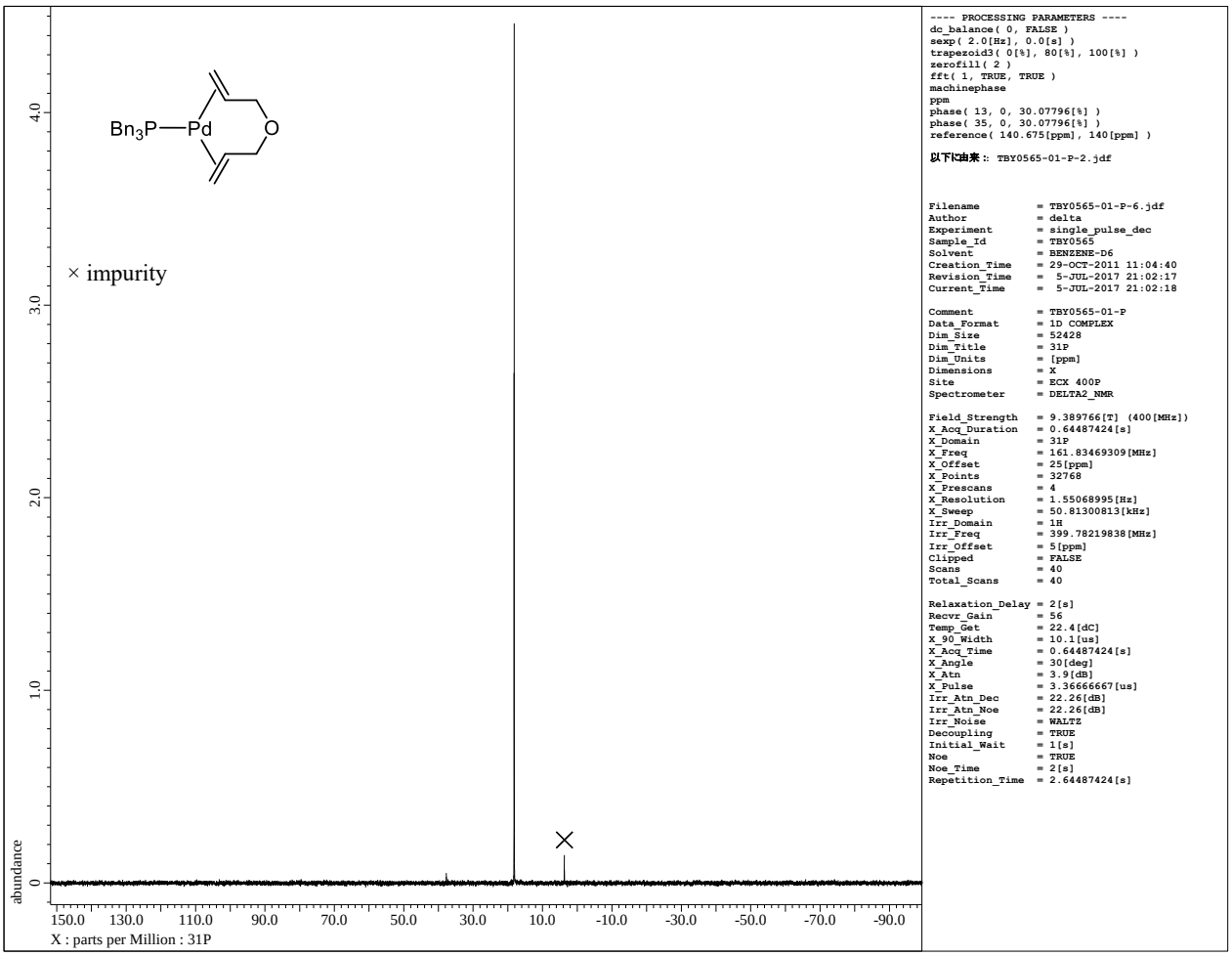

Figure S6. ^{31}P{^{1}H} NMR spectra of Pd(η^2,η^2-diallyl ether)(PBn_3) (**1-Bn**) (162 MHz, C_6D_6, 22 °C).

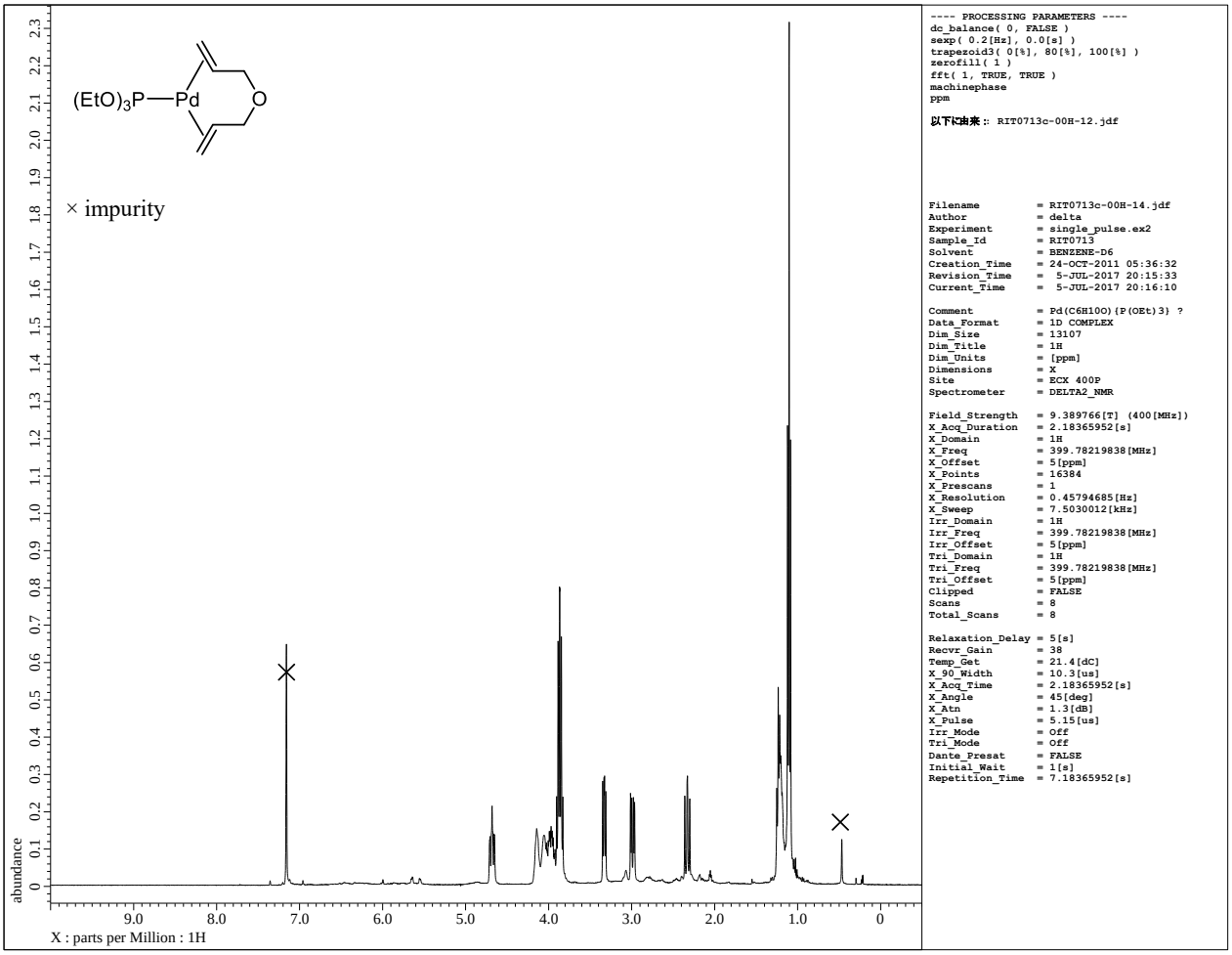

Figure S7. ^{1}H NMR spectra of Pd(η^2,η^2-diallyl ether){P(OEt)$_3$} (**1-OEt**) (400 MHz, C_6D_6, 21 °C).

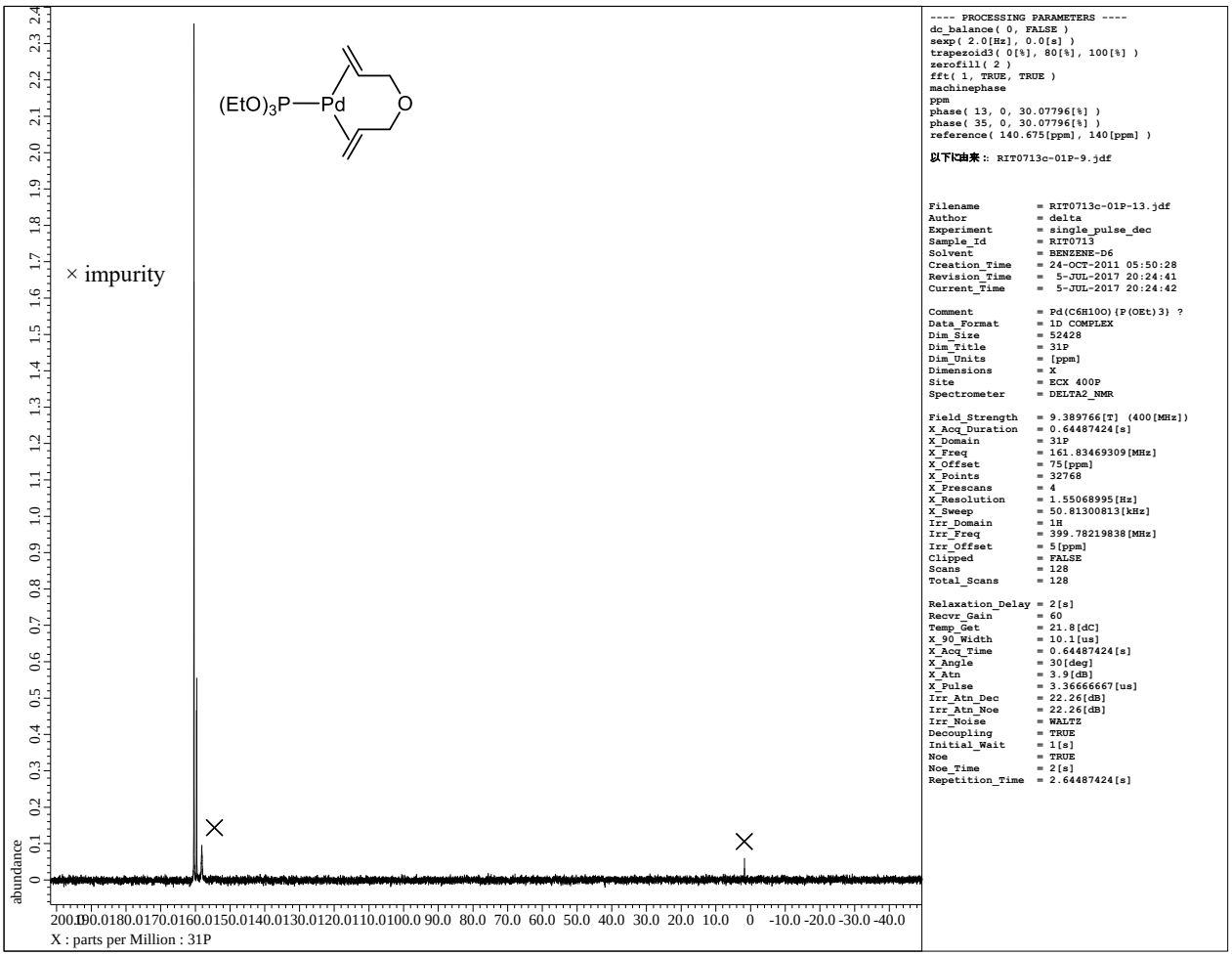

Figure S8. ^{31}P{^{1}H} NMR spectra of Pd(η^2,η^2-diallyl ether){P(OEt)$_3$} (**1-OEt**) (162 MHz, C_6D_6, 22 °C).

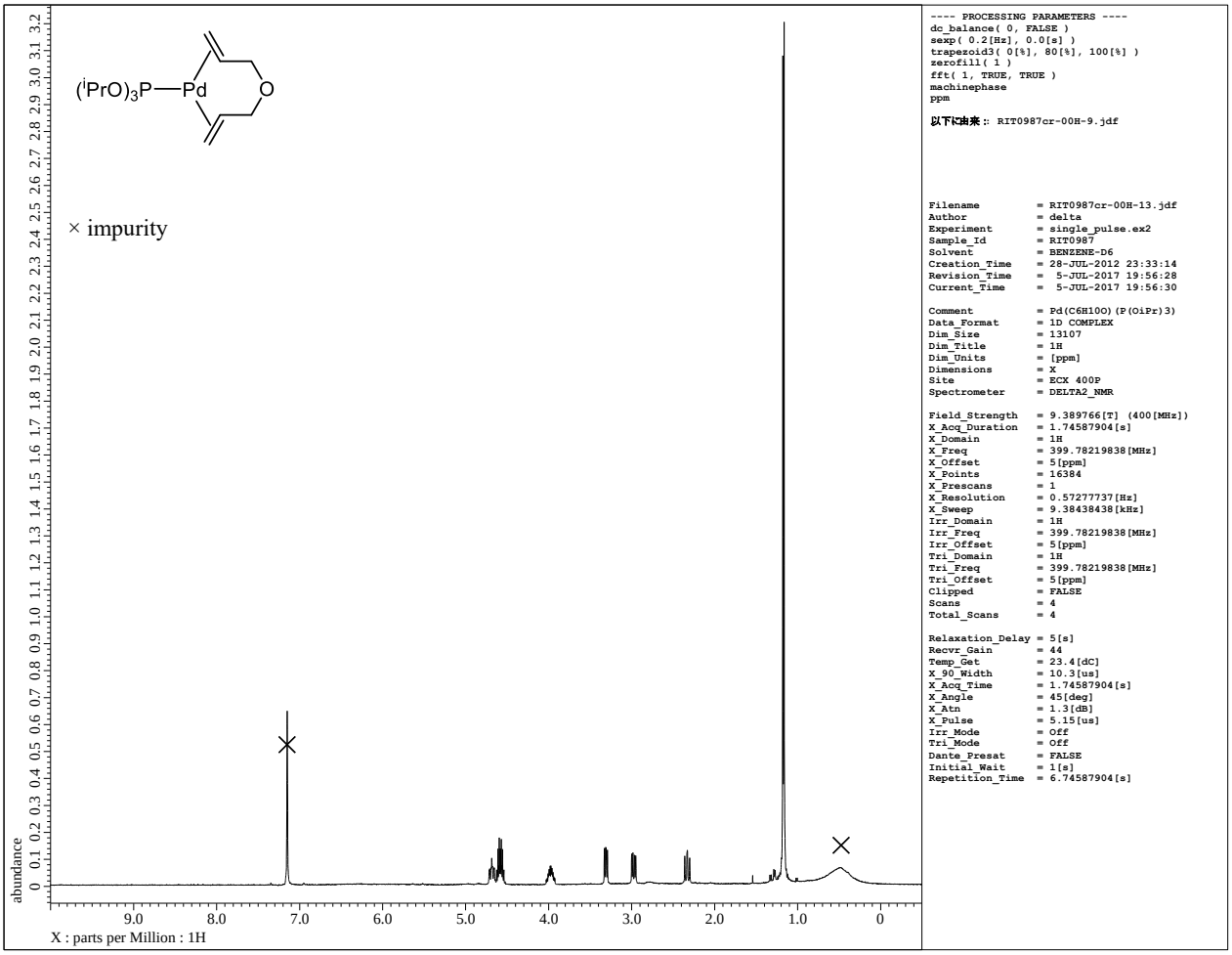

Figure S9. ^{1}H NMR spectra of Pd(η^2,η^2-diallyl ether){P(OiPr)$_3$} (**1-OiPr**) (400 MHz, C_6D_6, 23 °C).

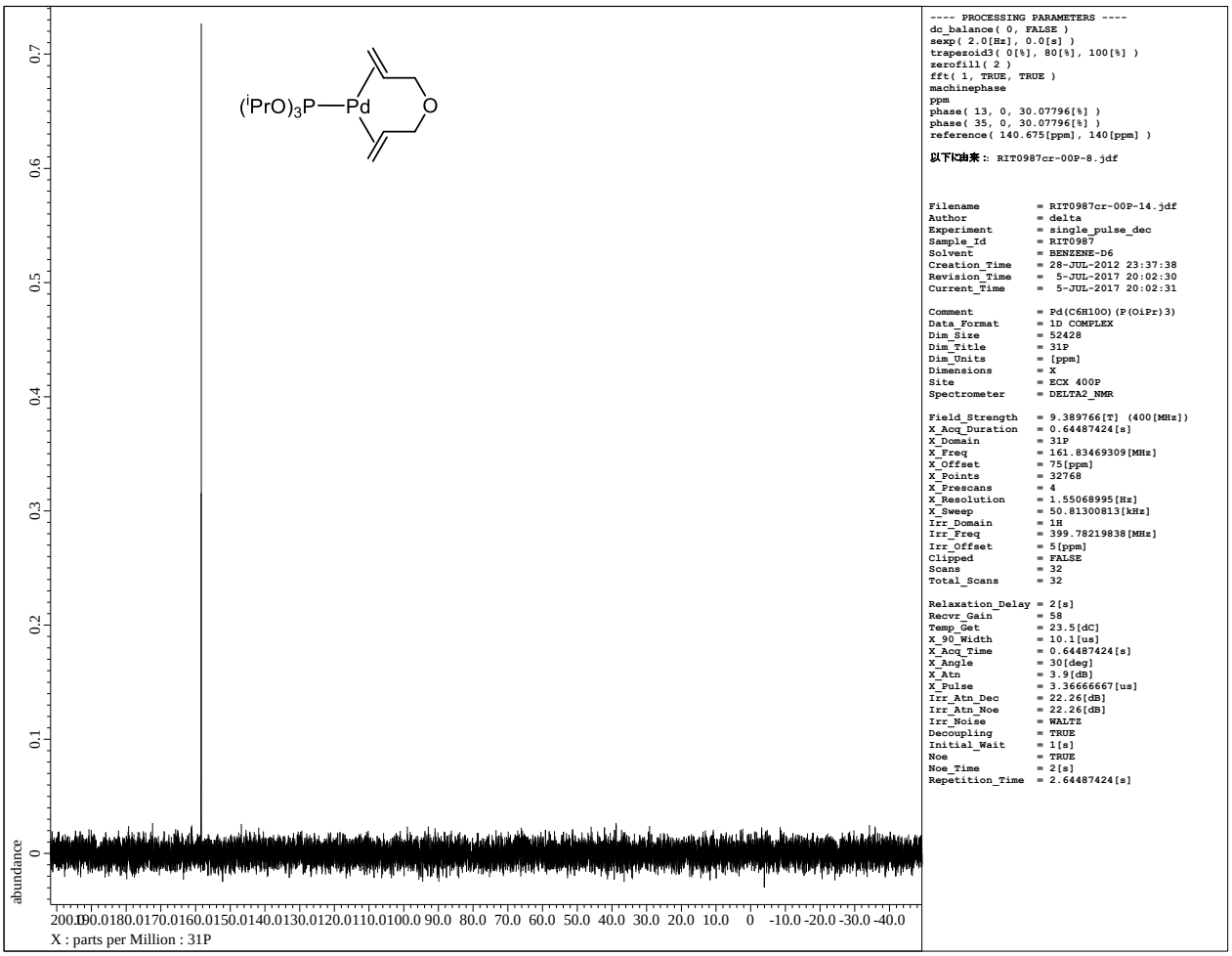

Figure S10. $^{31}P\{^{1}H\}$ NMR spectra of Pd(η^2,η^2-diallyl ether){P(OiPr)$_3$} (**1-OiPr**) (162 MHz, C_6D_6, 22 °C)

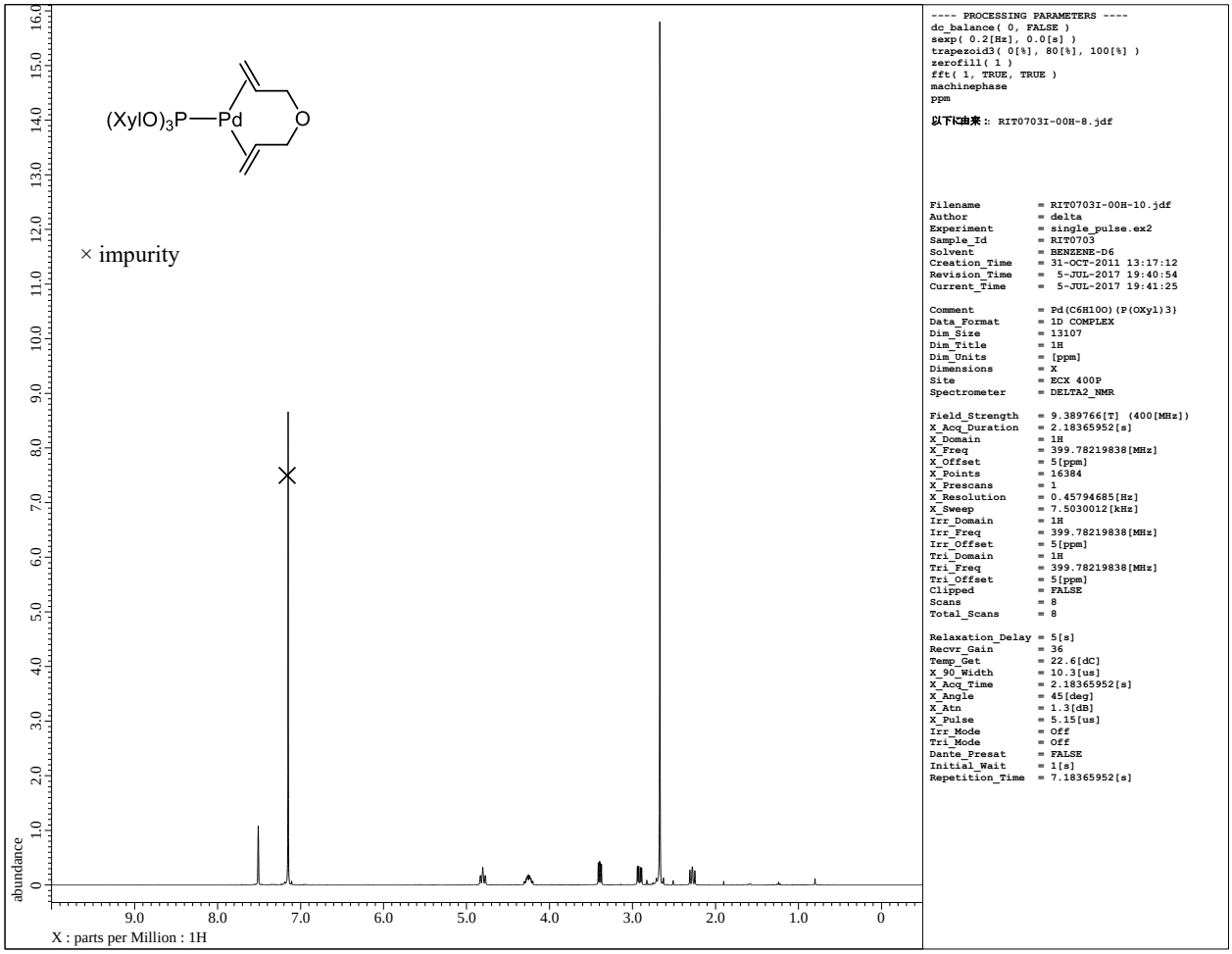

Figure S11. ^{1}H NMR spectra of Pd(η^2,η^2-diallyl ether){P(OXyl)$_3$} (**1-OXyl**) (400 MHz, C_6D_6, 23 °C)

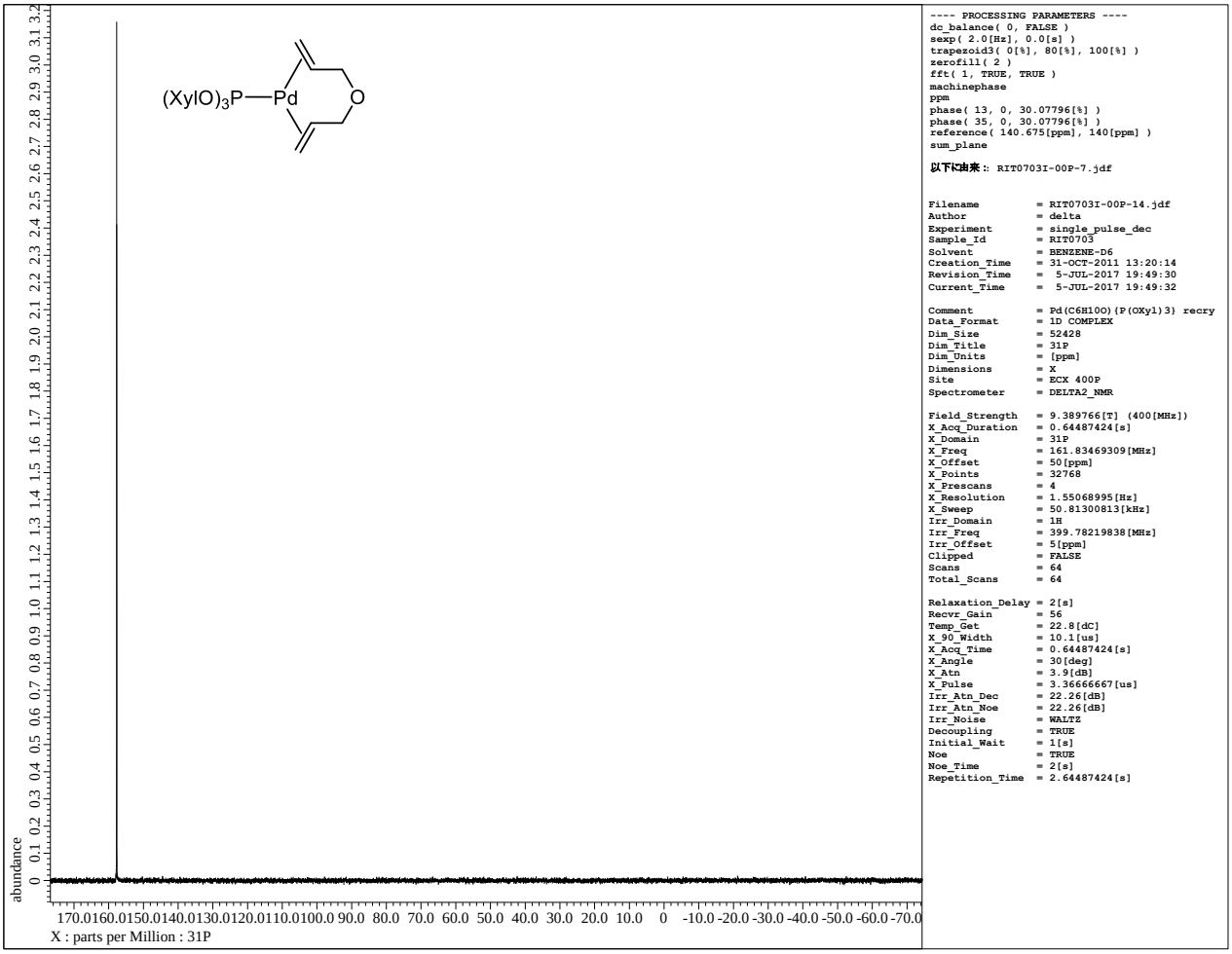

Figure S12. ^{31}P{^{1}H} NMR spectra of Pd(η^2,η^2-diallyl ether){P(OXyl)$_3$} (**1-OXyl**) (162 MHz, C_6D_6, 23 °C)

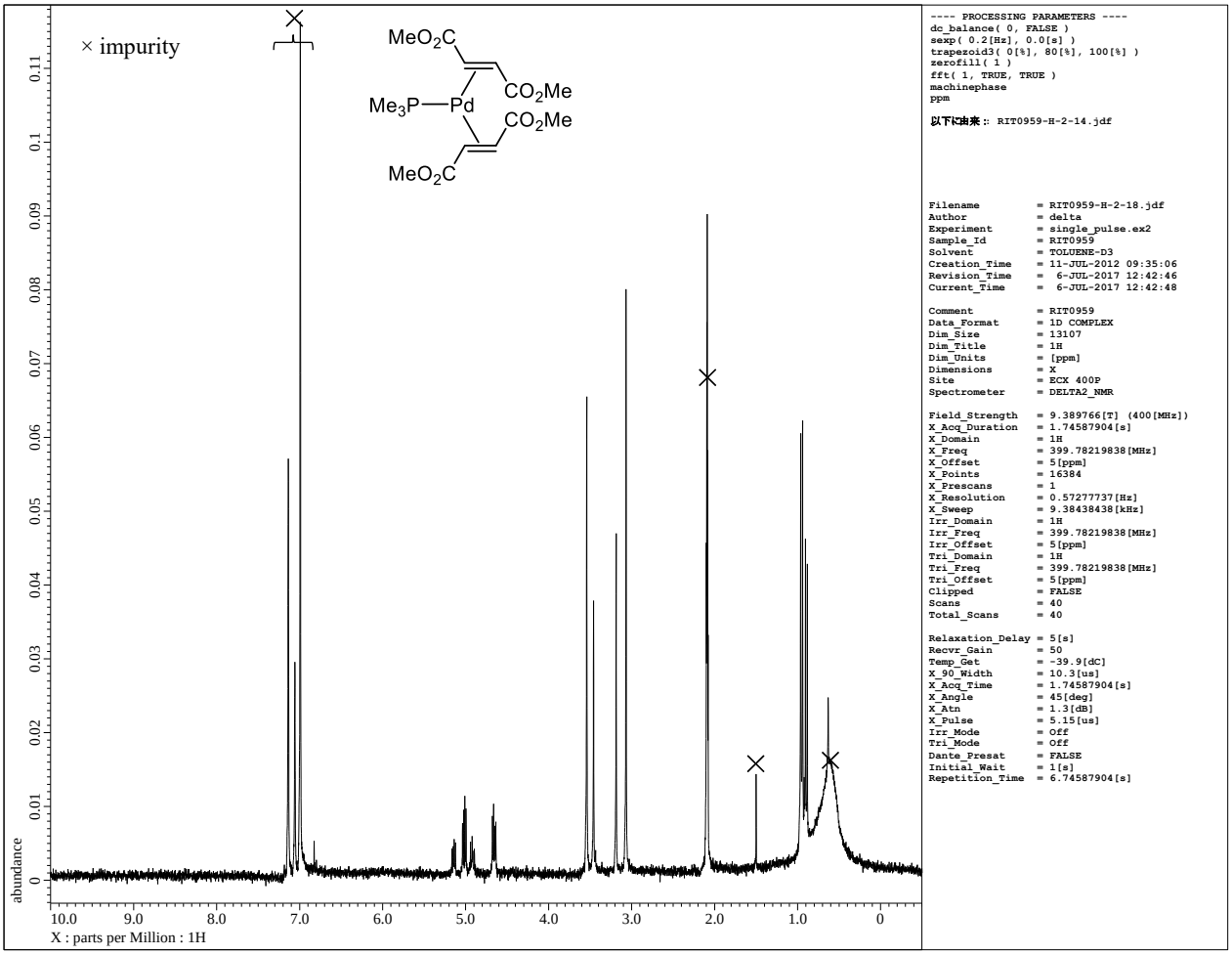

Figure S13. ^{1}H NMR spectra of Pd(η^2-dimethyl fumarate)$_2$(PMe$_3$) (**P1-Me**) (400 MHz, tolunene-d$_8$, -40 °C).

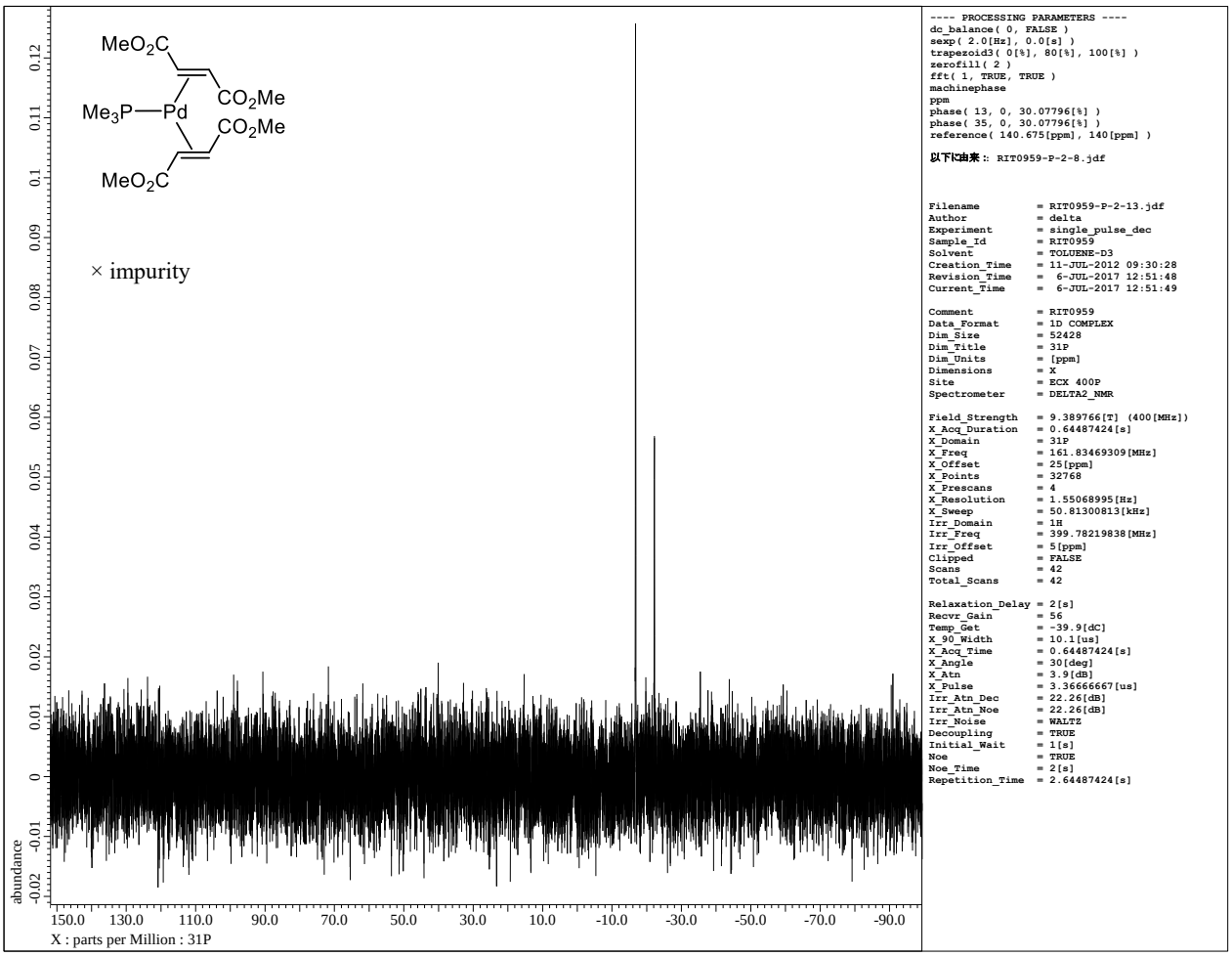

Figure S14. ^{31}P{^{1}H} NMR spectra of Pd(η^2-dimethyl fumarate)$_2$(PMe$_3$) (**P1-Me**) (162 MHz, tolunene-d$_8$, -40 °C).

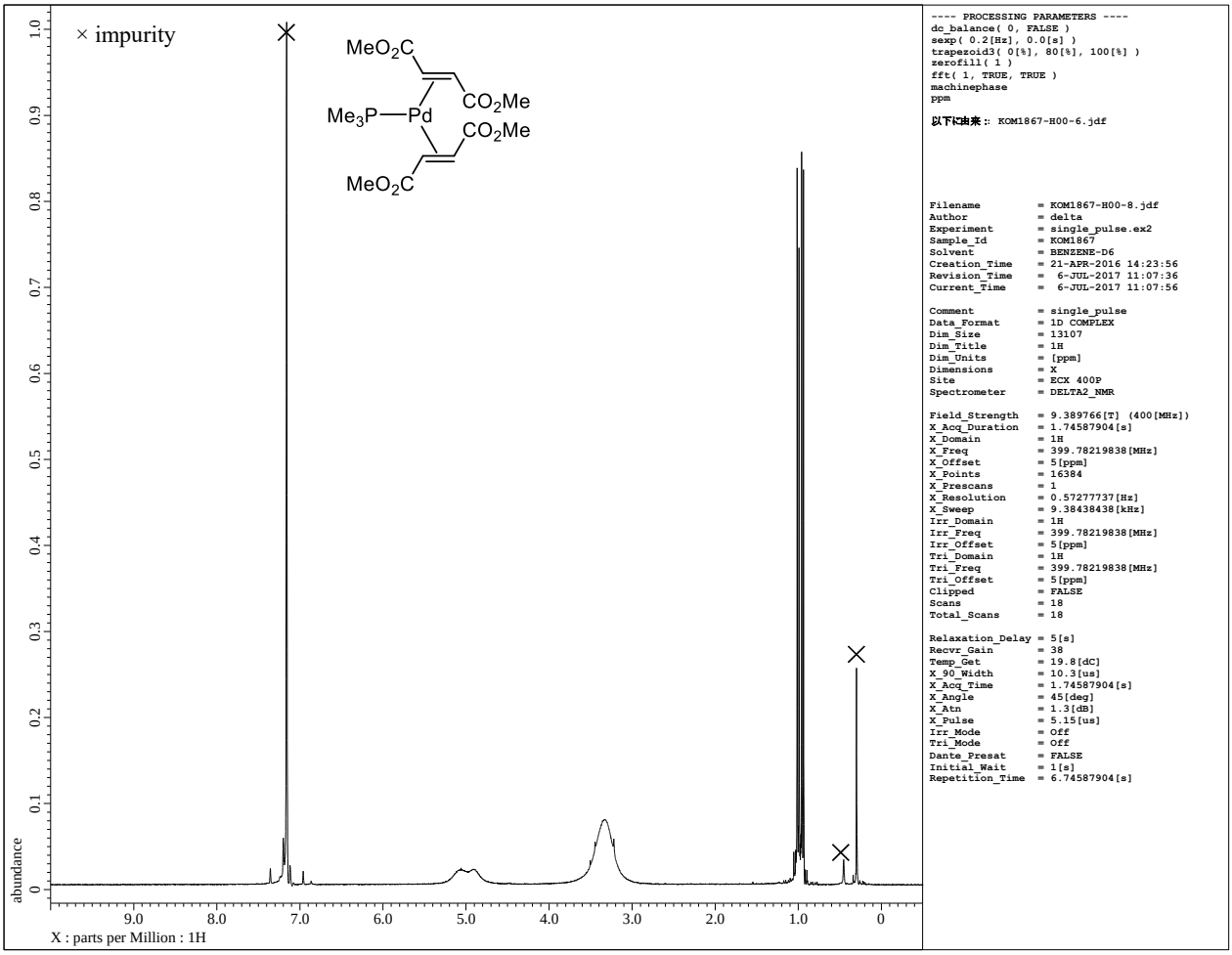

Figure S15. ^{1}H NMR spectra of Pd(η^2-dimethyl fumarate)$_2$(PMe$_3$) (**P1-Me**) (400 MHz, C_6D_6, 20 °C).

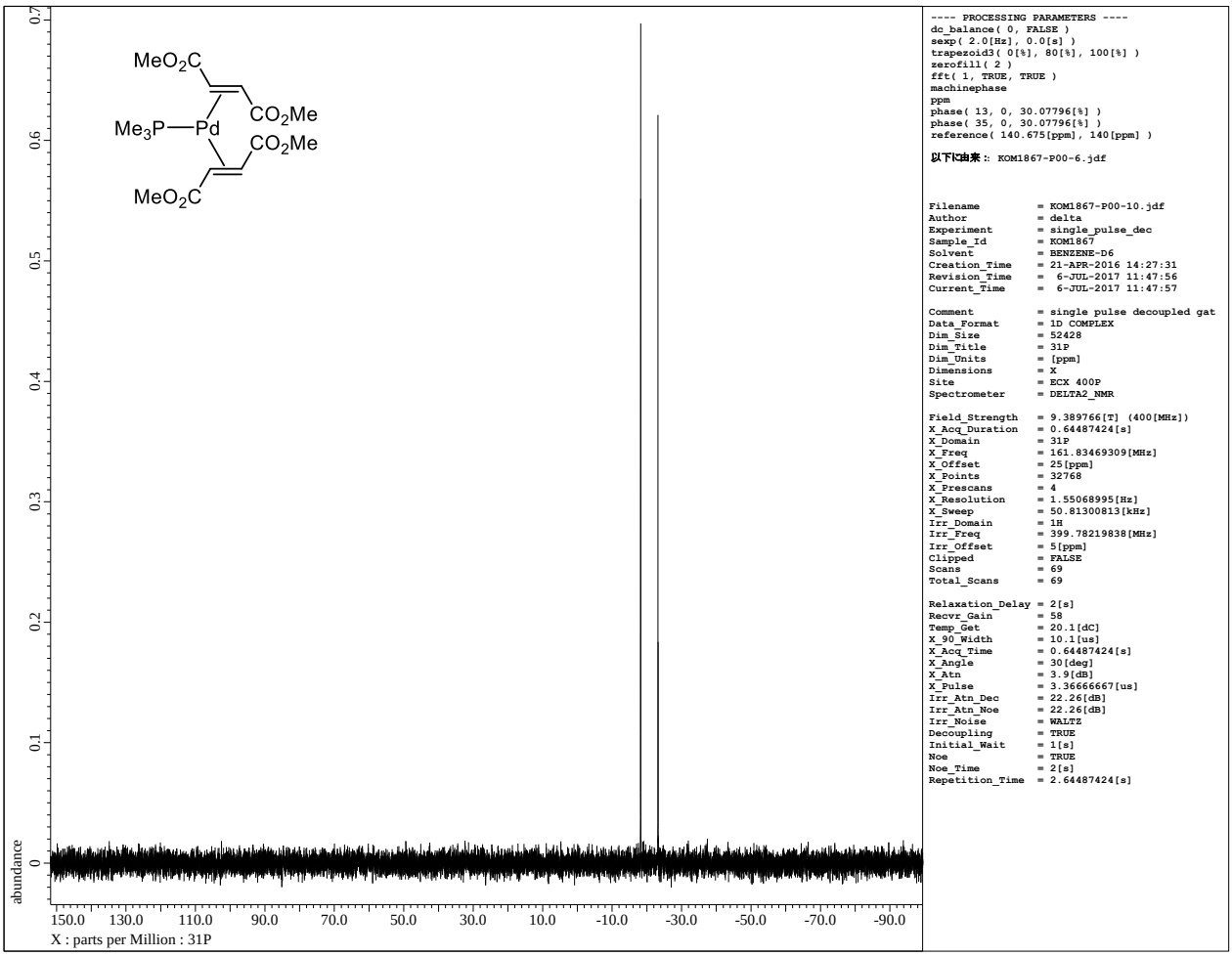

Figure S16. ^{31}P{^{1}H} NMR spectra of Pd(η^2-dimethyl fumarate)$_2$(PMe$_3$) (**P1-Me**) (162 MHz, C_6D_6, 20 °C).

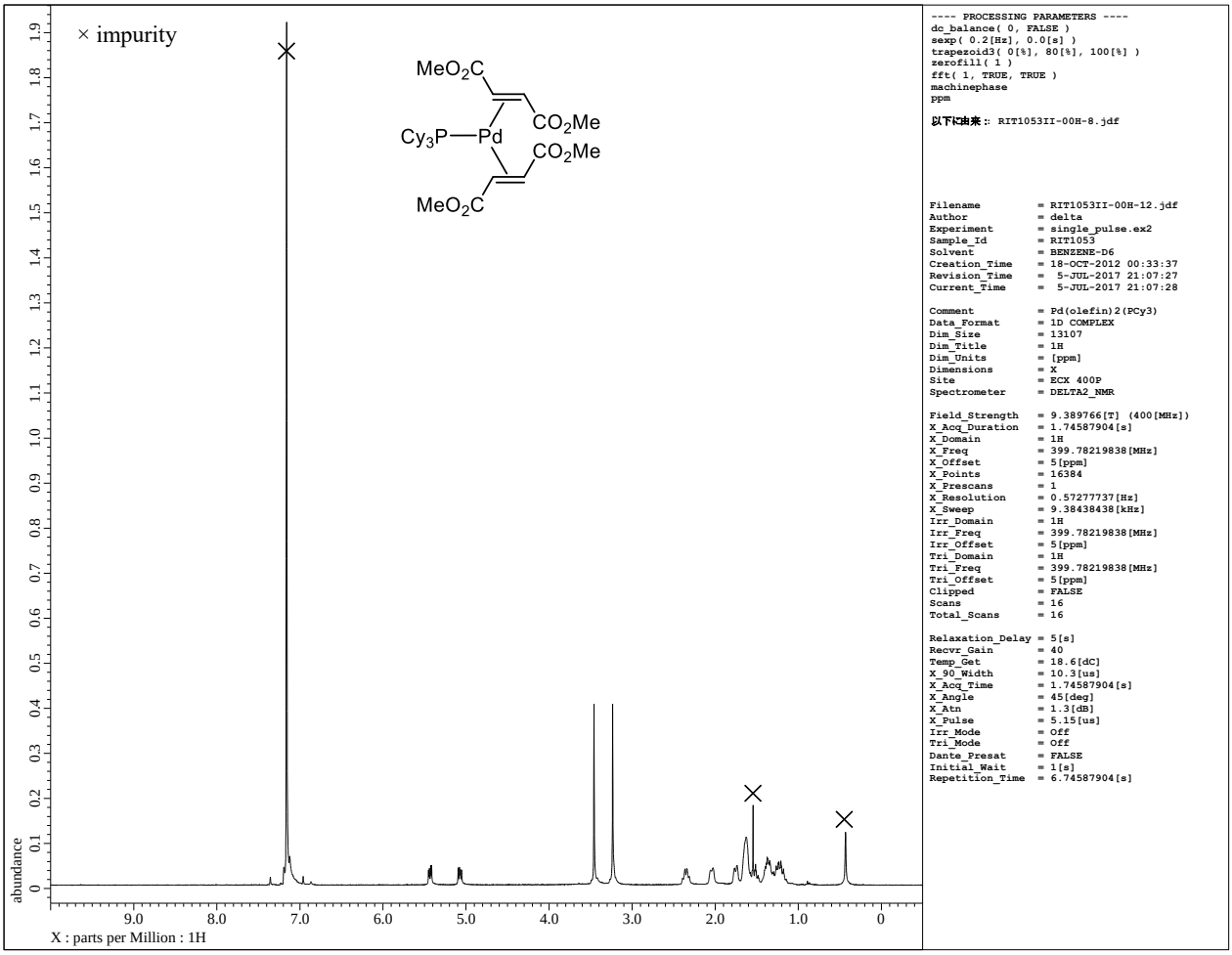

Figure S17. ^{1}H NMR spectra of Pd(η^2-dimethyl fumarate)$_2$(PCy_3) (**P1-Cy**) (400 MHz, C_6D_6, 19 °C).

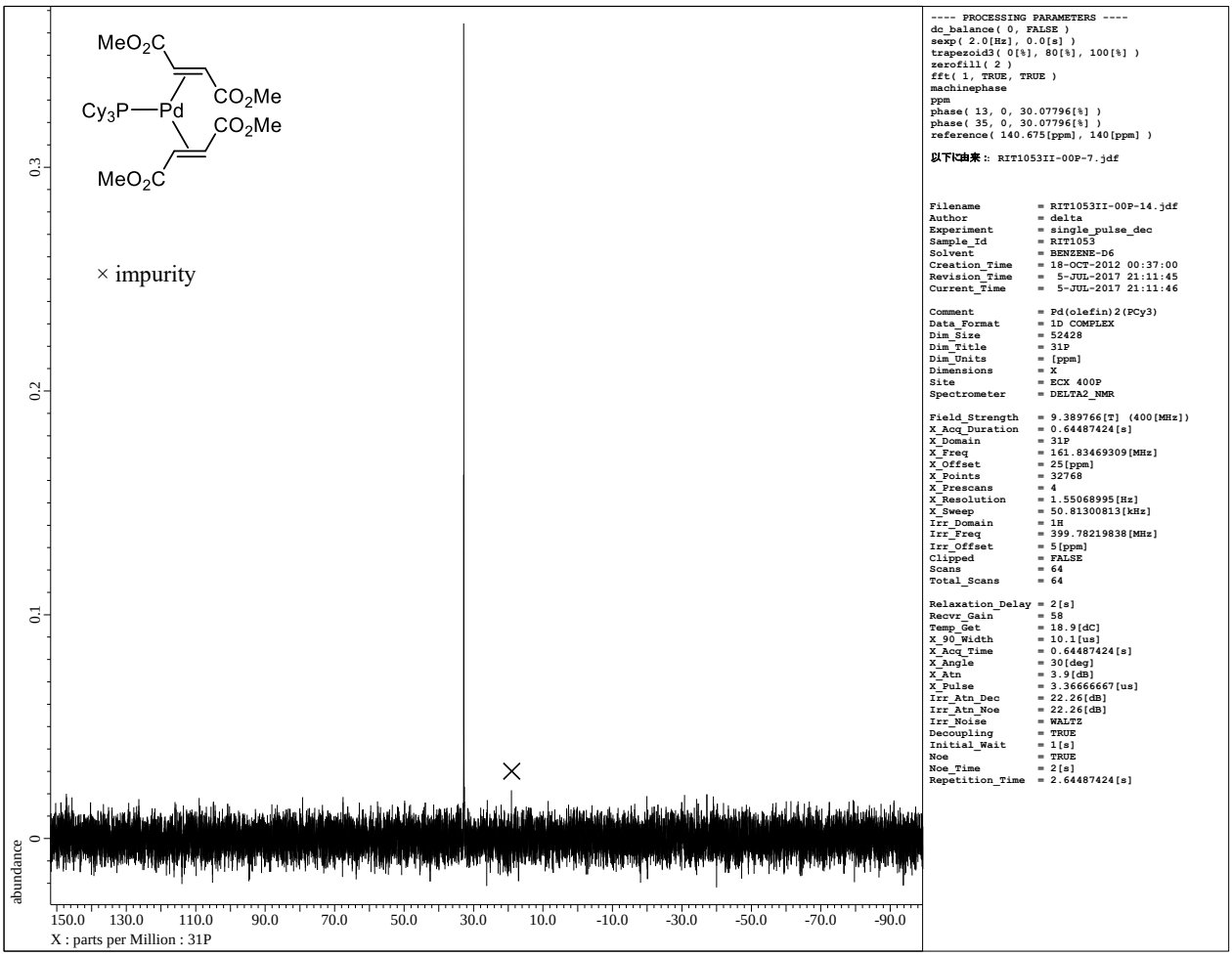

Figure S18. $^{31}P\{^{1}H\}$ NMR spectra of Pd(η^2-dimethyl fumarate)$_2$(PCy_3) (**P1-Cy**) (162 MHz, C_6D_6, 19 °C).

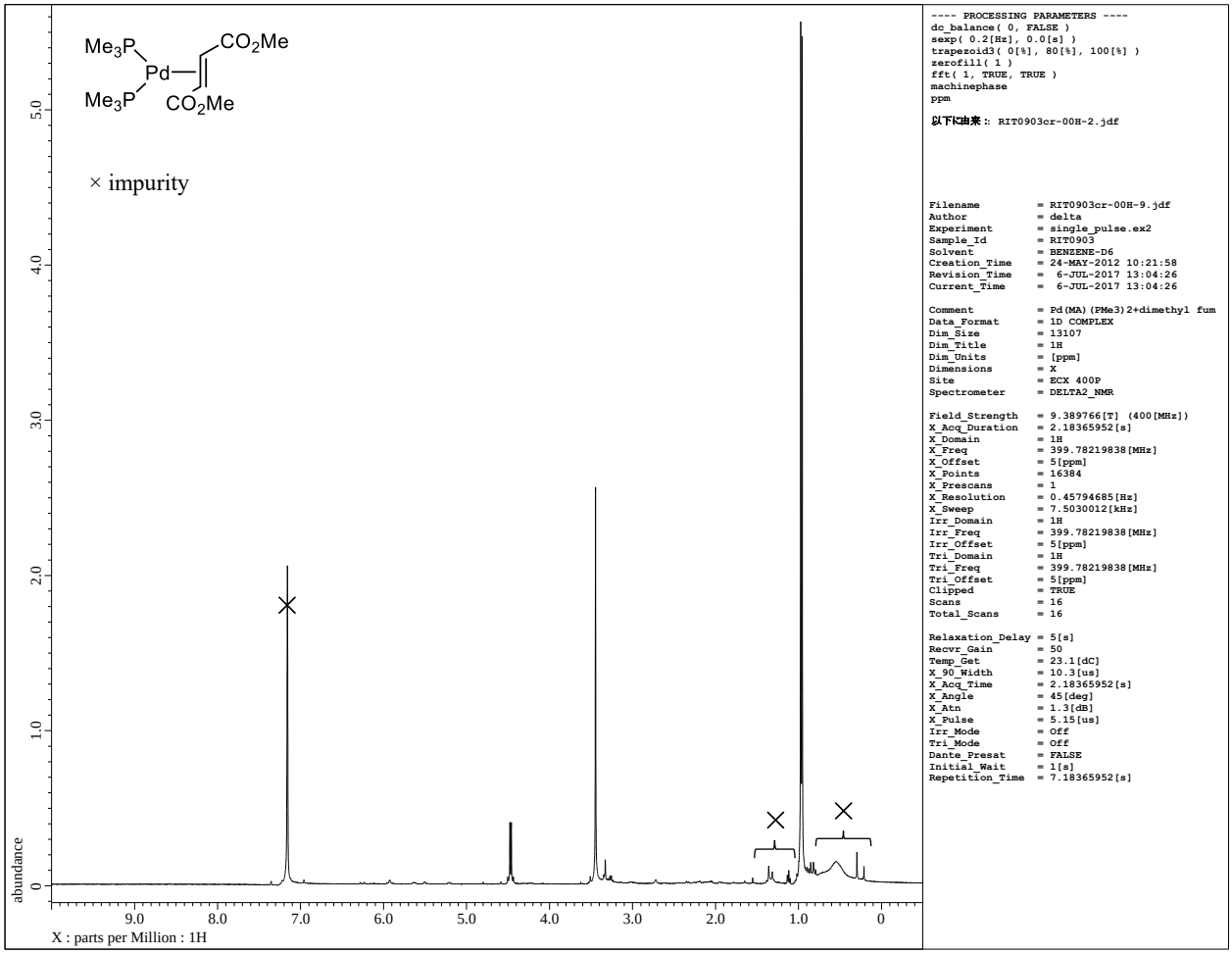

Figure S19. ^{1}H NMR spectra of Pd(η^2-dimethyl fumarate)(PMe_3)$_2$ (**P2-Me**) (400 MHz, C_6D_6, 23 °C).

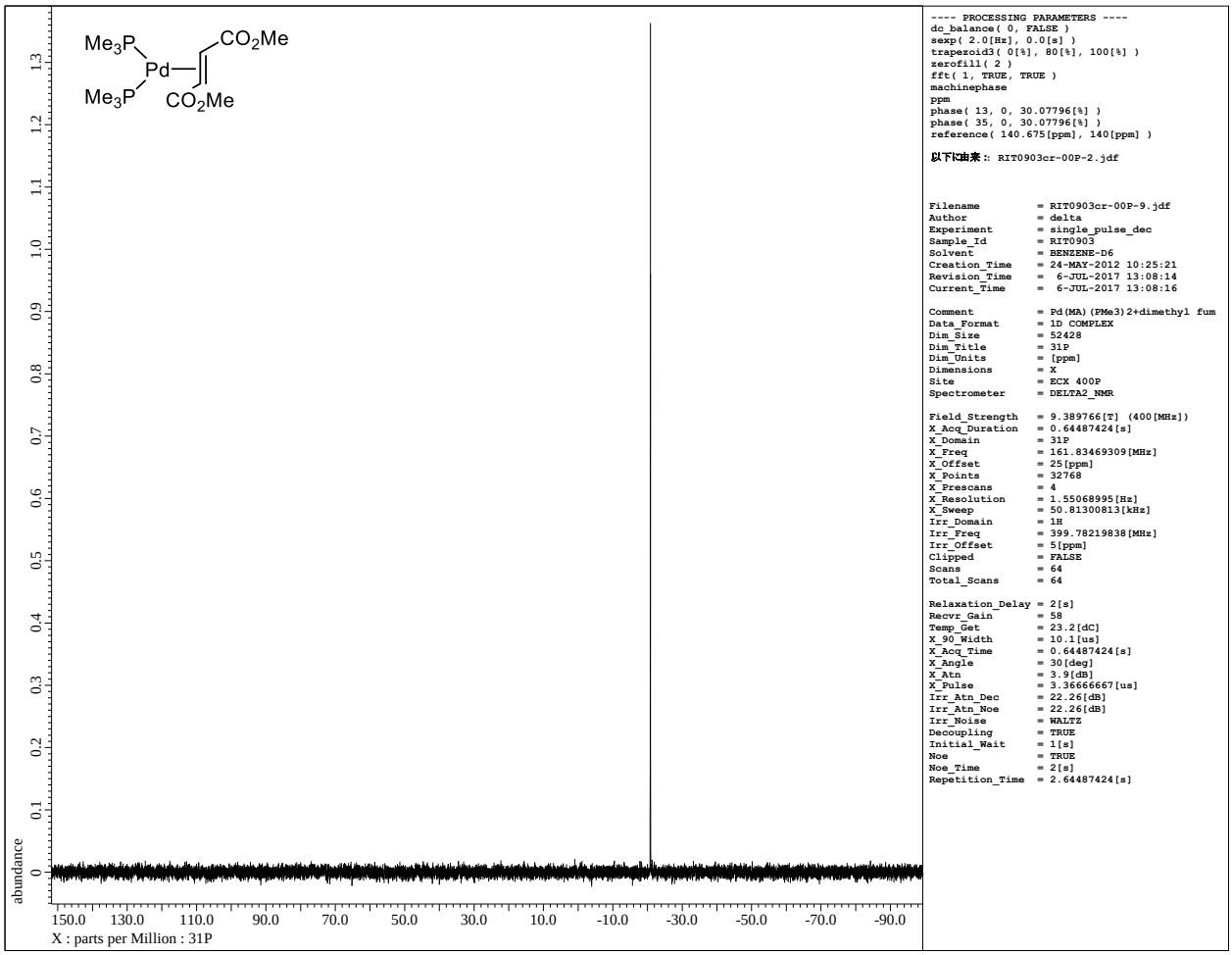

Figure S20. ^{31}P{^{1}H} NMR spectra of Pd(η^2-dimethyl fumarate)(PMe_3)$_2$ (**P2-Me**) (400 MHz, C_6D_6, 23 °C).

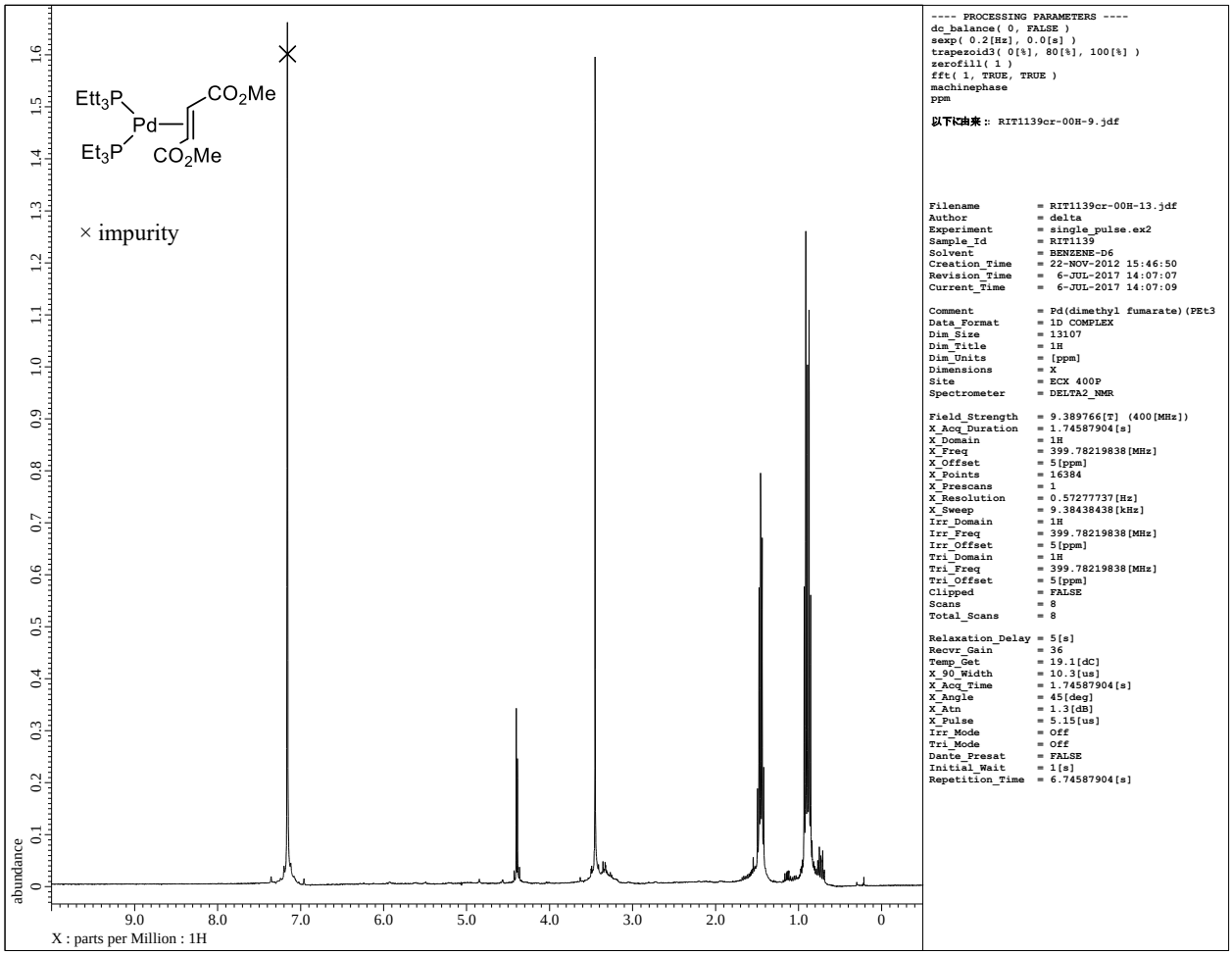

Figure S21. ^{1}H NMR spectra of Pd(η^2-dimethyl fumarate)(PEt_3)$_2$ (**P2-Et**) (400 MHz, C_6D_6, 19 °C).

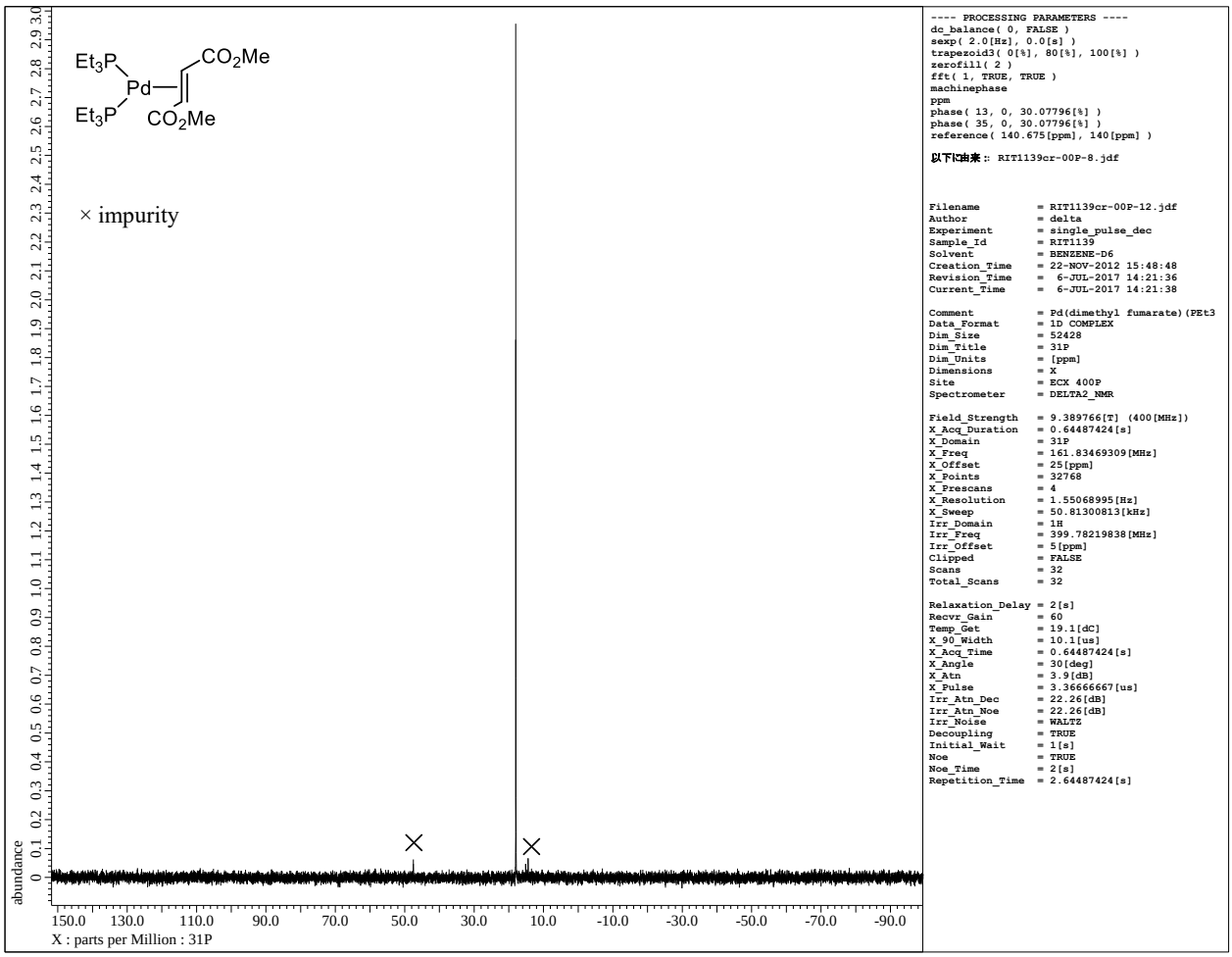

Figure S22. ^{31}P{^{1}H} NMR spectra of Pd(η^2-dimethyl fumarate)(PEt_3)$_2$ (**P2-Et**) (400 MHz, C_6D_6, 19 °C).

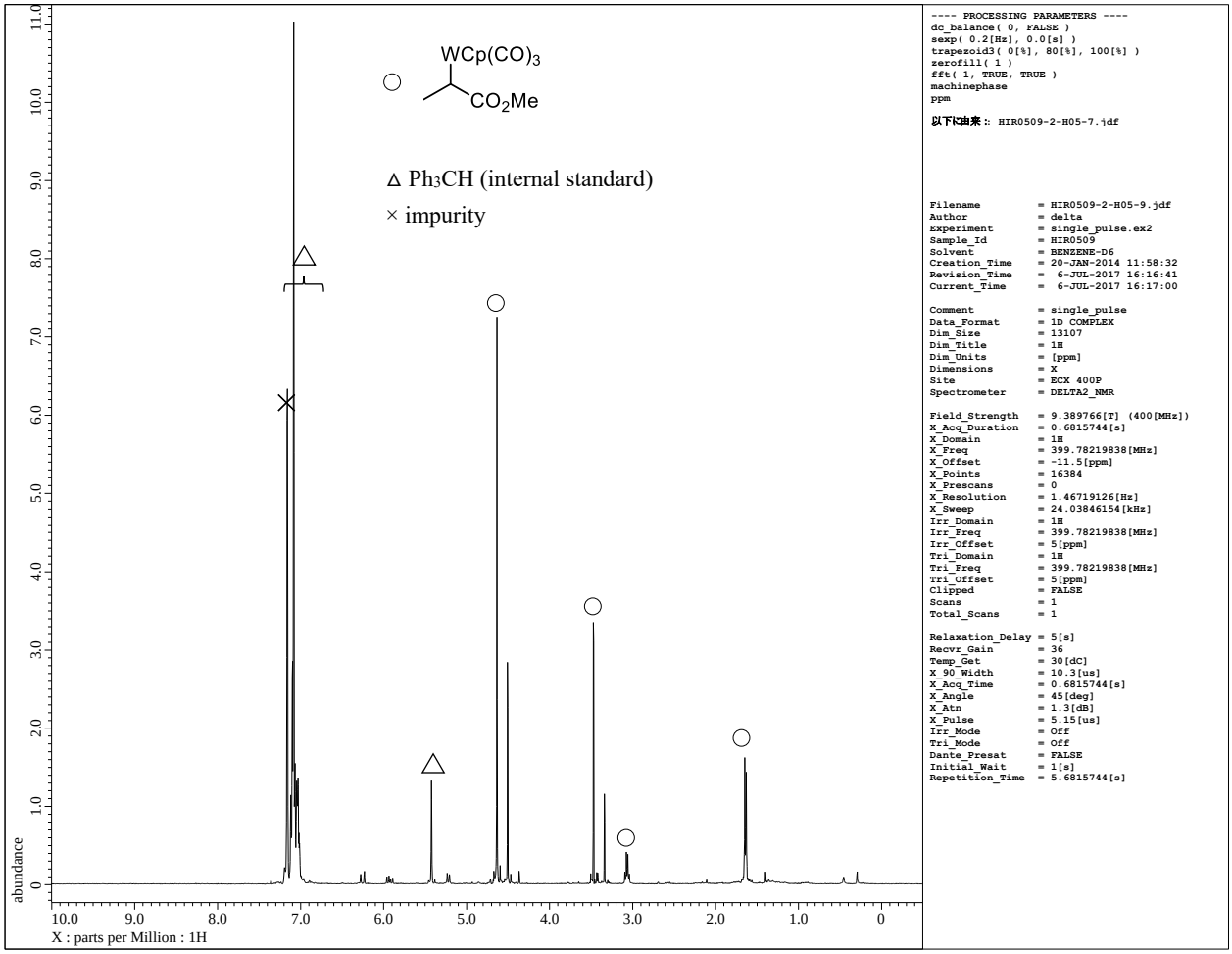

Figure S23. ^{1}H NMR spectra of catalytic reaction of $WHCp(CO)_3$ with methyl acrylate (400 MHz, C_6D_6, 30 °C).

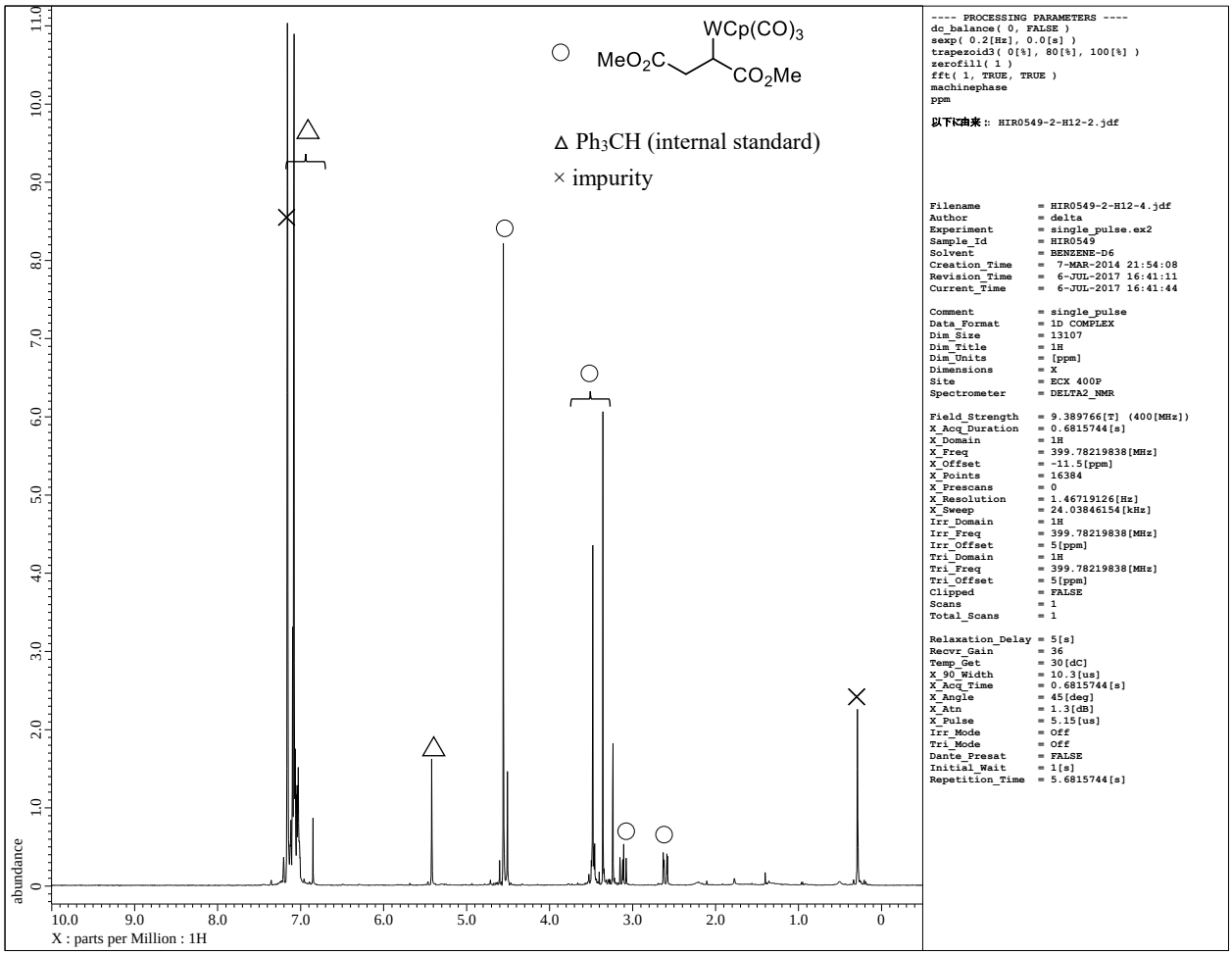

Figure S24. ^{1}H NMR spectra of catalytic reaction of $WHCp(CO)_3$ with dimethyl maleate (400 MHz, C_6D_6, 30 °C).

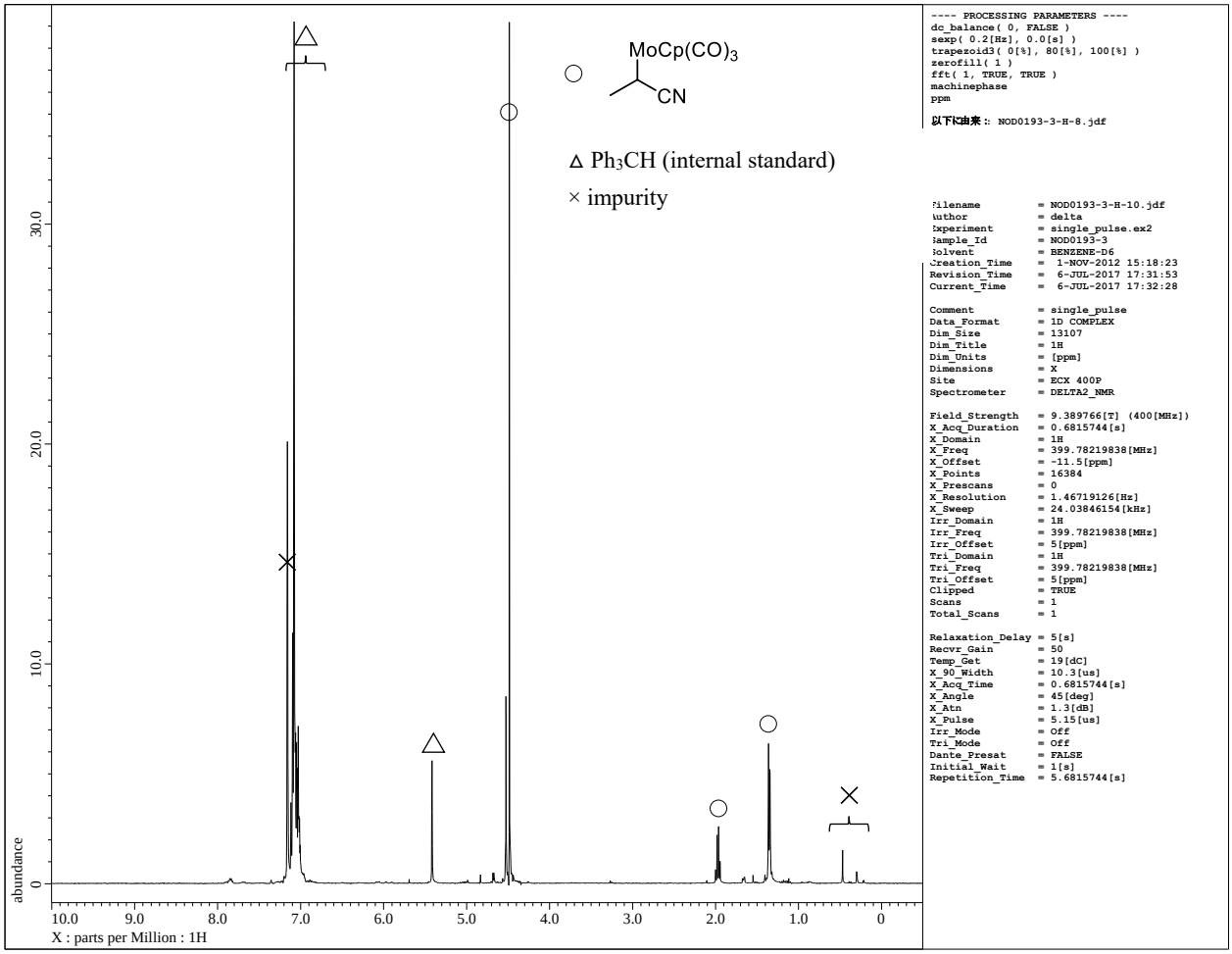

Figure S25. ^{1}H NMR spectra of catalytic reaction of $MoHCp(CO)_3$ with acrylonitrile (400 MHz, C_6D_6, 30 °C).

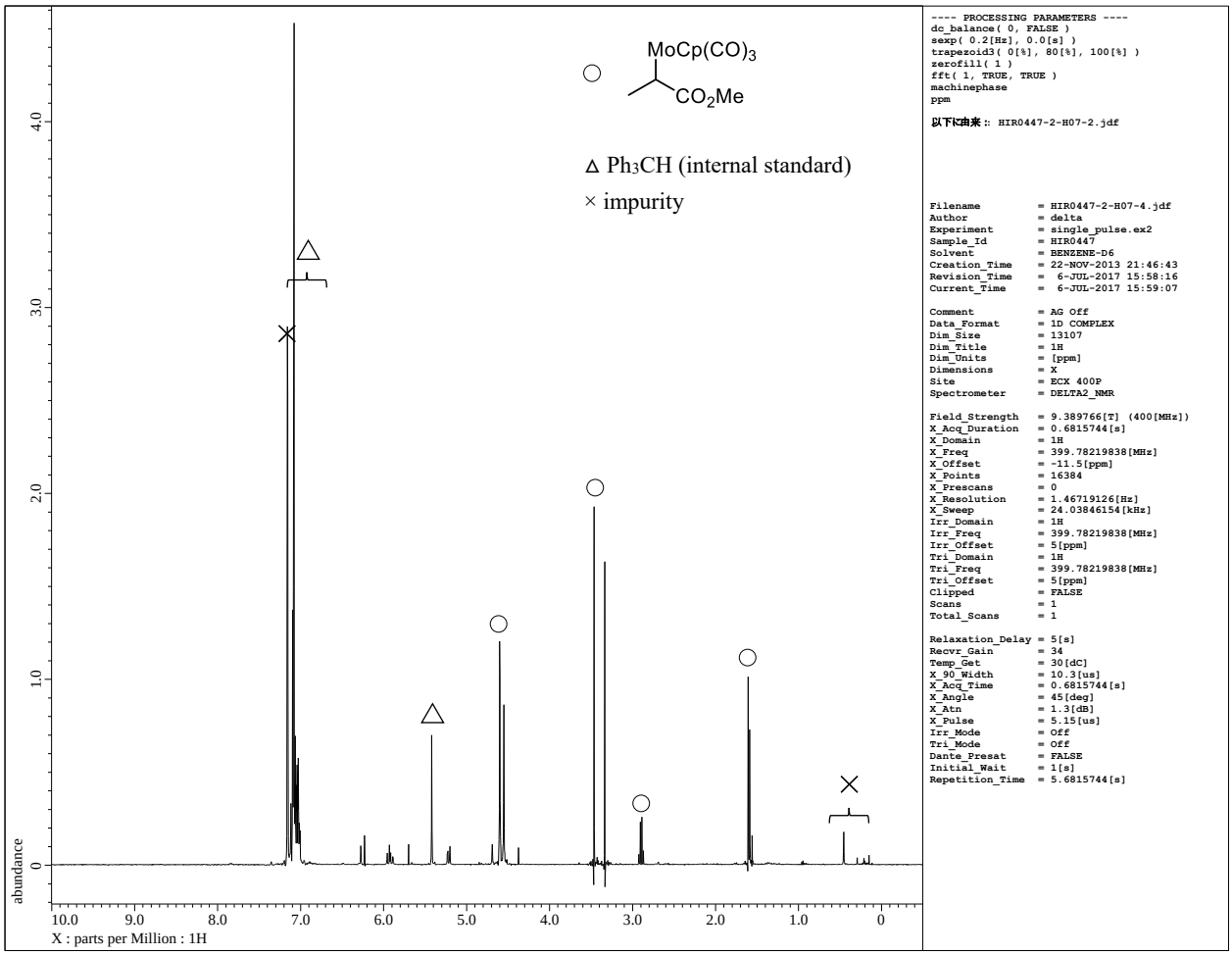

Figure S26. ^{1}H NMR spectra of catalytic reaction of $MoHCp(CO)_3$ with methyl acrylate (400 MHz, C_6D_6, 30 °C).

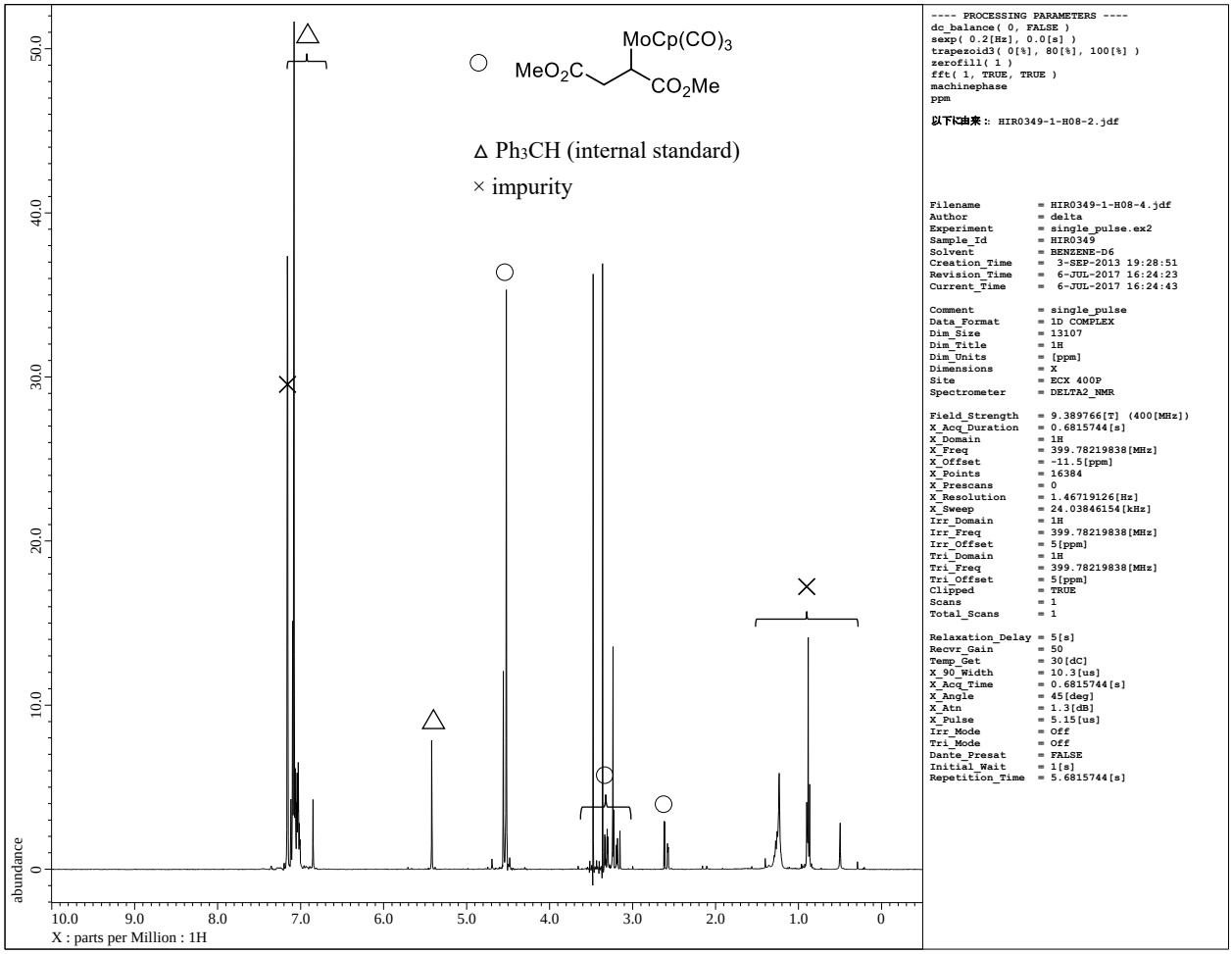

Figure S27. ^{1}H NMR spectra of catalytic reaction of $MoHCp(CO)_3$ with dimethyl maleate (400 MHz, C_6D_6, 30 °C).

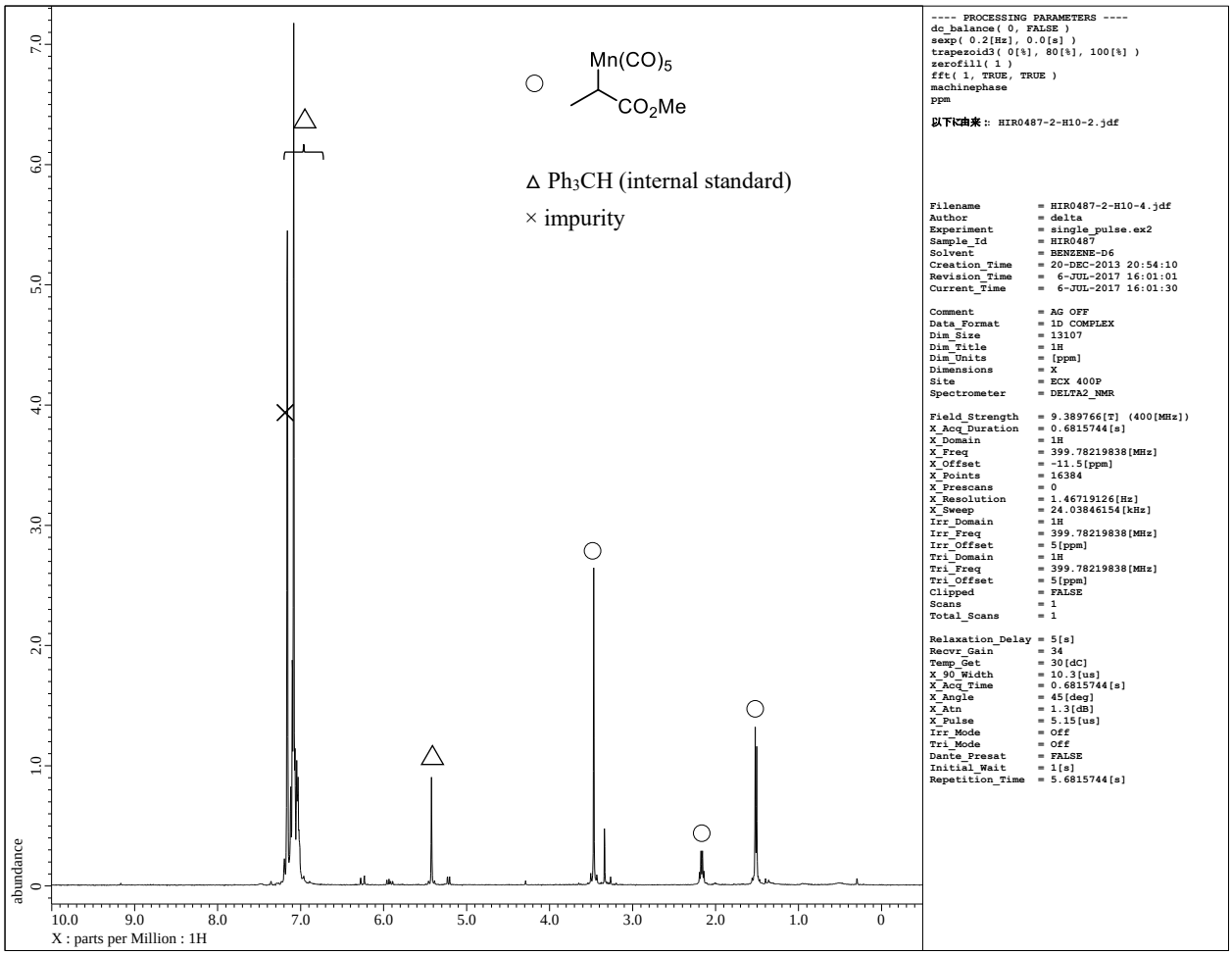

Figure S28. ^{1}H NMR spectra of catalytic reaction of $MnH(CO)_5$ with methyl acrylate (400 MHz, C_6D_6, 30 °C).

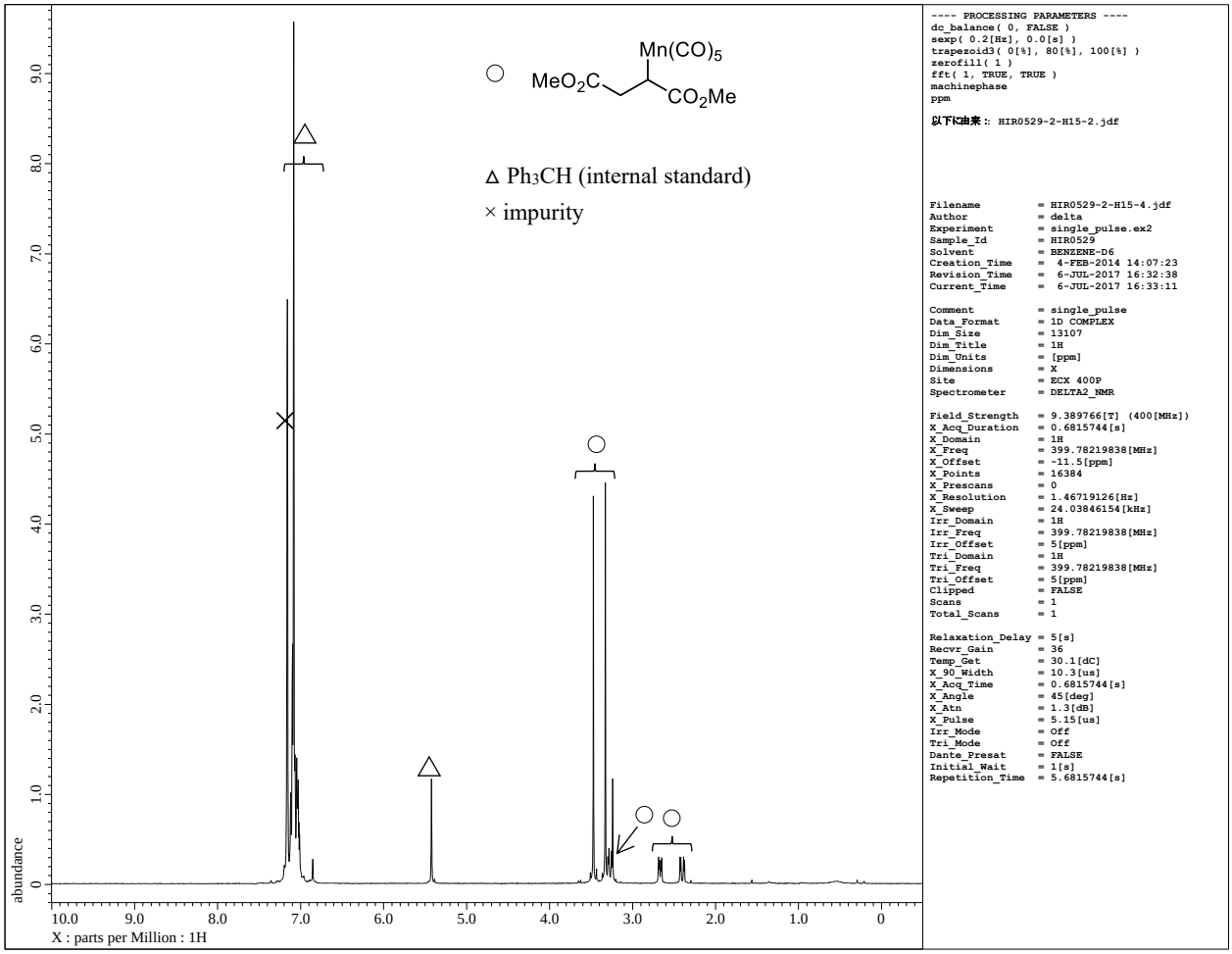

Figure S29. ^{1}H NMR spectra of catalytic reaction of $MnH(CO)_5$ with dimethyl maleate (400 MHz, C_6D_6, 30 °C).

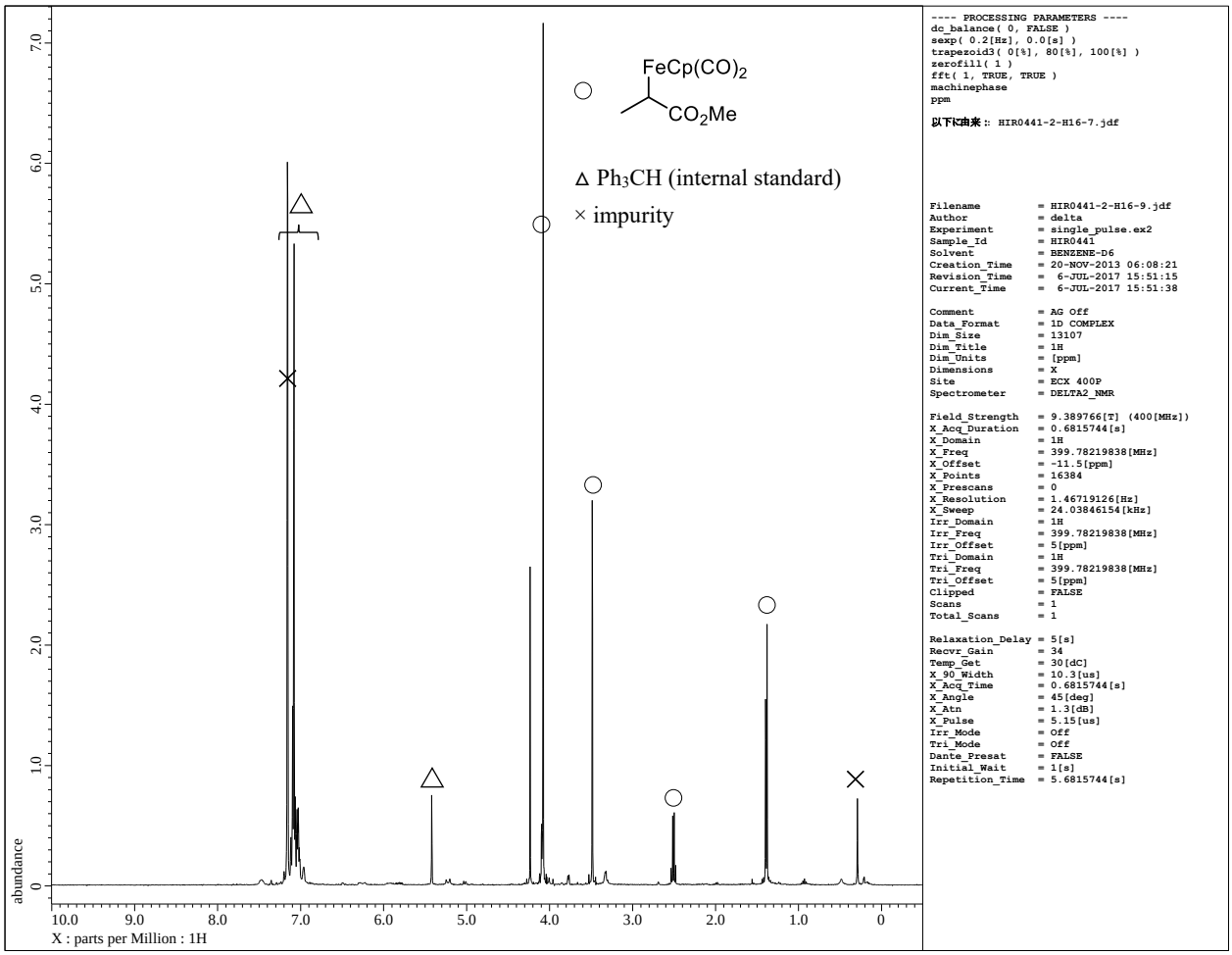

Figure S30. ^{1}H NMR spectra of catalytic reaction of $FeHCp(CO)_2$ with methyl acrylate (400 MHz, C_6D_6, 30 °C).

2. Kinetic data for catalytic reaction of $WHCp(CO)_3$ with dimethyl fumarate

(1) Dependence of initial reaction rate on on [Pd(dimethyl fumarate)$_2$(PMe_3)]$_0$. ([**4-Me**]$_0$)

Table S2. Reaction conditions and initial reaction rates.

Entry	10^2 [$WHCp(CO)_3$]$_0$/M	10^2 [dimethyl fumarate]/M	10^4 [**4-Me**]$_0$/M	10^6 V_0/M s^{-1}
1	3.60	3.74	1.24	2.66
2	3.62	3.62	3.64	7.04
3	3.59	3.65	5.38	9.26
4	3.58	3.97	7.36	13.14

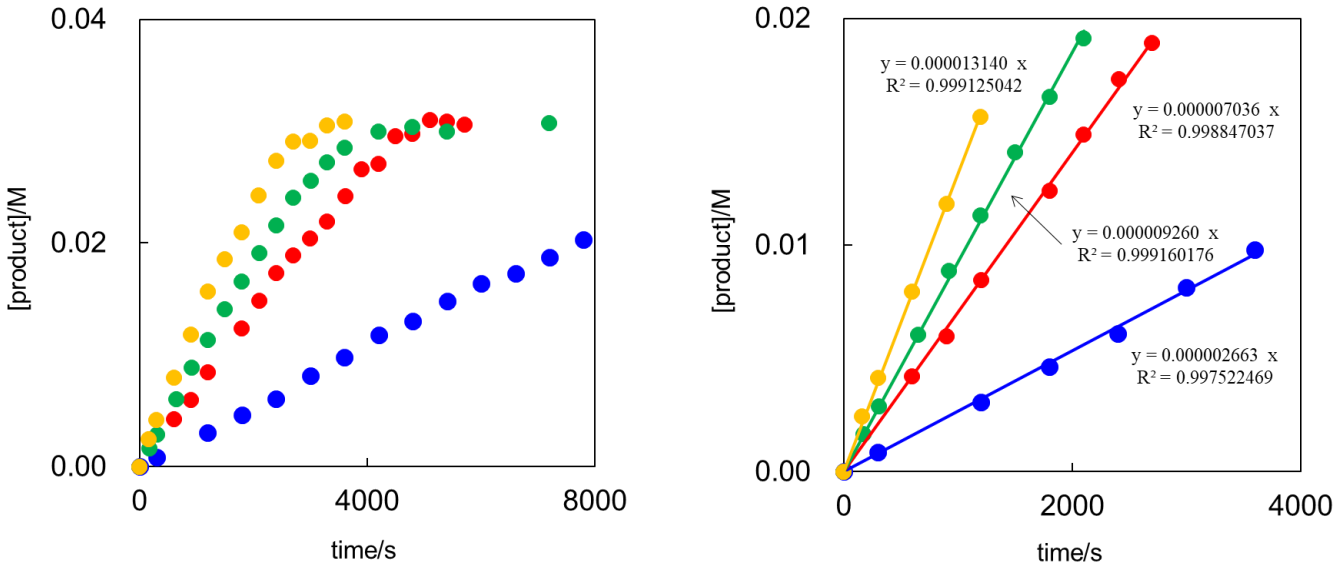

Figure S31. Time-courses of catalytic reactions: entry 1 (●), entry 2 (●), entry 3 (●), entry 4 (●).

(2) Dependence of initial reaction rate on on $[WHCp(CO)_3]_0$.

Table S3. Reaction conditions and initial reaction rates

Entry	10^2 $[WHCp(CO)_3]_0$/M	10^2 [dimethyl fumarate]/M	10^4 [**4-Me**]$_0$/M	10^6 V_0/M s^{-1}
1	1.64	3.88	3.90	3.11
3	2.50	3.76	3.58	6.29
4	4.38	3.88	3.90	10.70
5	5.59	3.54	3.62	16.13

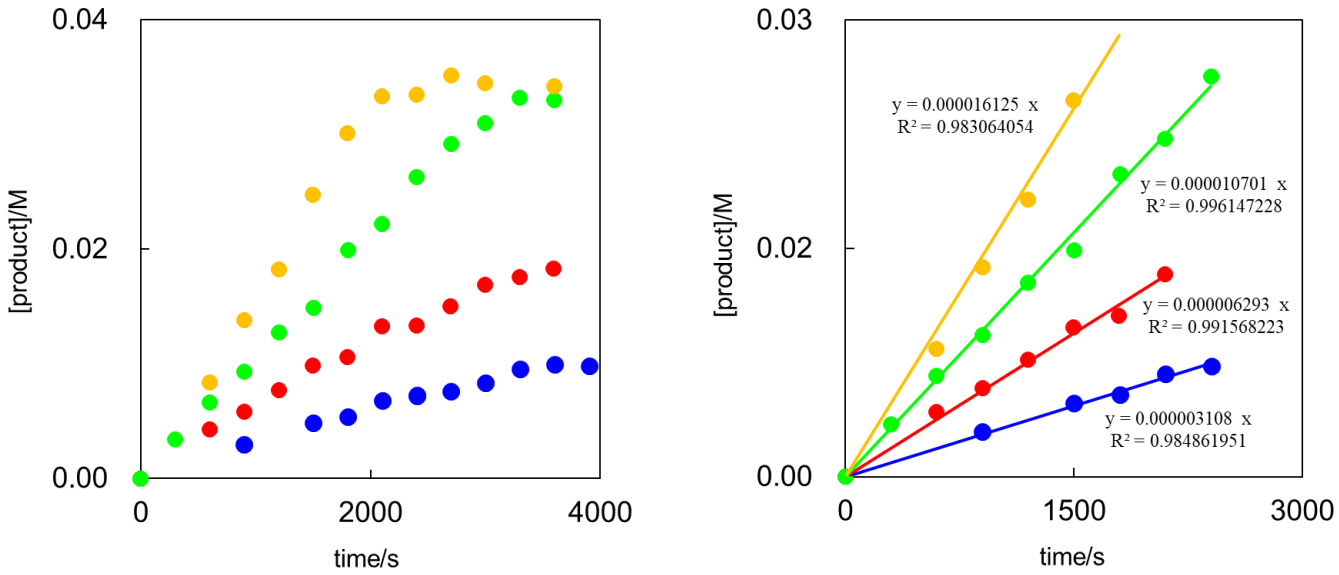

Figure S32. Time-courses of catalytic reactions: entry 1 (●), entry 2 (●), entry 3 (●), entry 4 (●).

(3) Dependence of initial reaction rate on [dimethyl fumarate]$_0$.

Table S4. Reaction conditions and initial reaction rates.

Entry	10^2 [$WHCp(CO)_3$]$_0$/M	10^2 [dimethyl fumarate]/M	[dimethyl fumarate]$^{-1}$/M^{-1}	10^4 [**4-Me**]$_0$/M	10^6 V_0/M s^{-1}
1	3.62	3.62	26.23	3.63	7.04
2	3.62	4.36	22.92	3.67	6.14
3	3.61	6.75	14.81	3.68	3.37
4	3.66	10.99	9.10	3.64	2.17
5	3.62	16.95	5.90	3.66	1.44

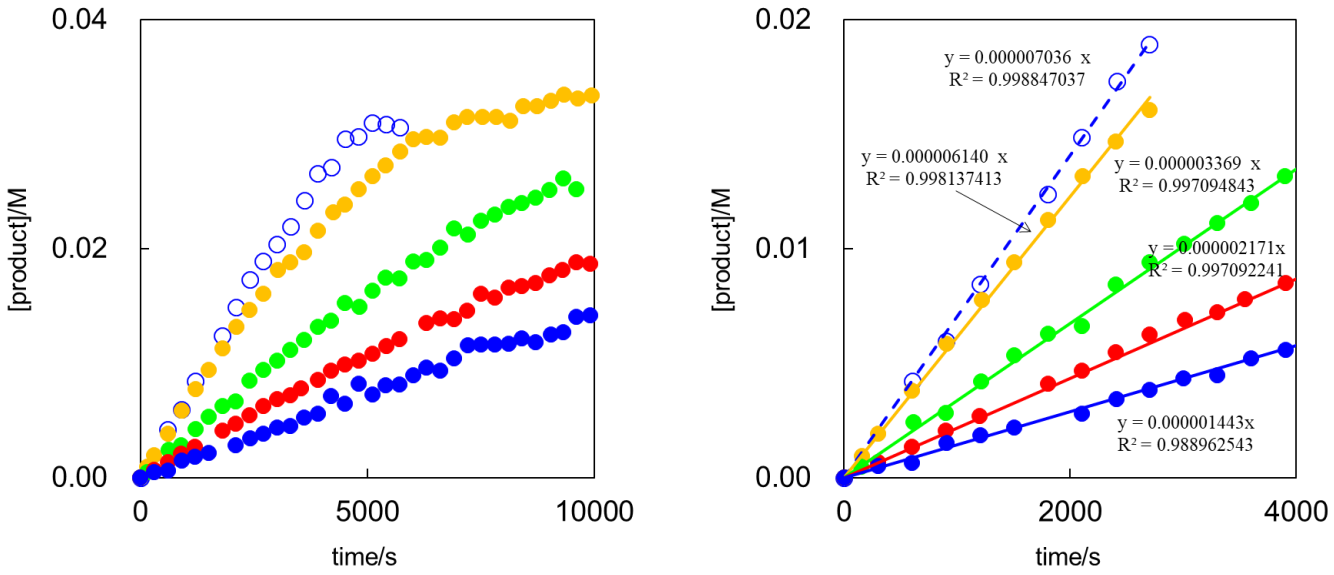

Figure S33. Time-courses of catalytic reactions: entry 1 (●), entry 2 (●), entry 3 (●), entry 4 (●), entry 5 (○).

(4) Dependence of initial reaction rate on temperature.

Table S5. Reaction conditions, initial reaction rates and rate constants.

Entry	Temp./°C	10^2 [$WHCp(CO)_3$]$_0$ /M	10^2 [dimethyl fumarate]$_0$/M	10^4 [**4-Me**]$_0$/M	10^6 V_0/M s^{-1}
1	10	3.63	19.6	3.77	0.466
2	20	3.66	19.5	3.65	1.39
3	30	3.66	19.5	3.65	3.85
4	40	3.60	19.0	3.72	9.44
5	50	3.61	19.2	3.61	18.7

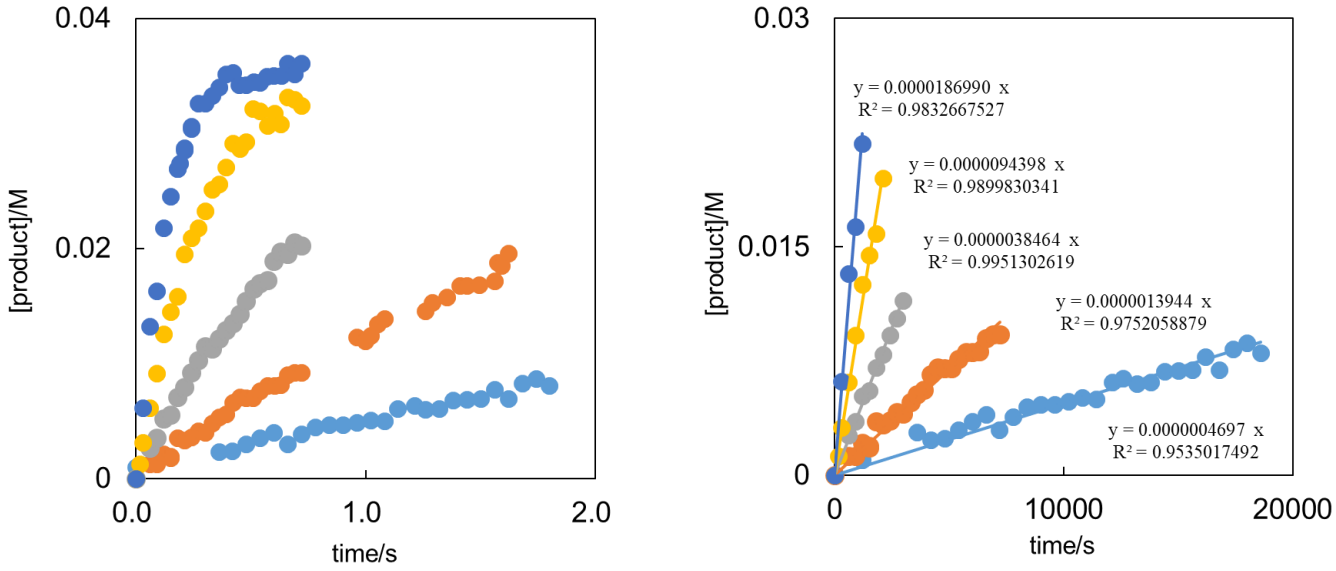

Figure S34. Time-courses of catalytic reactions: entry 1 (●), entry 2 (●), entry 3 (●), entry 4 (●), entry 5 (●).

(5) Eyring Plot

Table S6. Data for Eyring plot.

Entry	Temp. /°C	10^3 T^{-1} /K^{-1}	10^6 V_0/M s^{-1}	10^2 k_{obs}[a]/s^{-1}	ln(k_{obs}/T)
1	10	3.531697	0.466	0.667	-10.65617523
2	20	3.411223	1.39	2.03	-9.575412042
3	30	3.298697	3.85	5.63	-8.591379597
4	40	3.193358	9.44	13.4	-7.758437273
5	50	3.094538	18.7	27.6	-7.066318615

a) k_{obs} = V_0 [dimethyl fumarate]$_0$/([**4-Me**]$_0$ [WHCp(CO)$_3$]$_0$) from eq. 6 in main text.

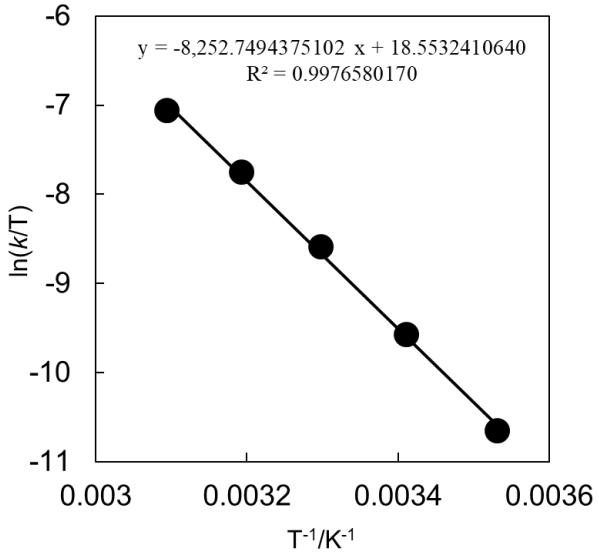

Figure S35. Eyring plot for insertion of dimethyl fumarate into WHCp(CO)$_3$ catalyzed by **4-Me.**

Eyring equation: $\ln\frac{k}{T} = \frac{-\Delta H^{\ddagger}}{R}\frac{1}{T} + \ln\frac{k_B}{h} + \frac{\Delta S^{\ddagger}}{R}$

$\frac{-\Delta H^{\ddagger}}{R}$ = 8252.749438±230.8548775 K^{-1}, $\Delta H^{\ddagger}$ = 68.6±2.2 kJ mol^{-1}

$\ln\frac{k_B}{h} + \frac{\Delta S^{\ddagger}}{R}$ = 18.55324106±0.764017541, $\Delta S^{\ddagger}$ = -43.3±7.3 J mol^{-1} K^{-1}

$\Delta G^{\ddagger} = \Delta H^{\ddagger} - T\Delta S^{\ddagger}$, $\Delta G^{\ddagger}$(25 °C) = 81.5±3.8 kJ mol^{-1}

2. Rate equation

Scheme S1. Possible mechanism

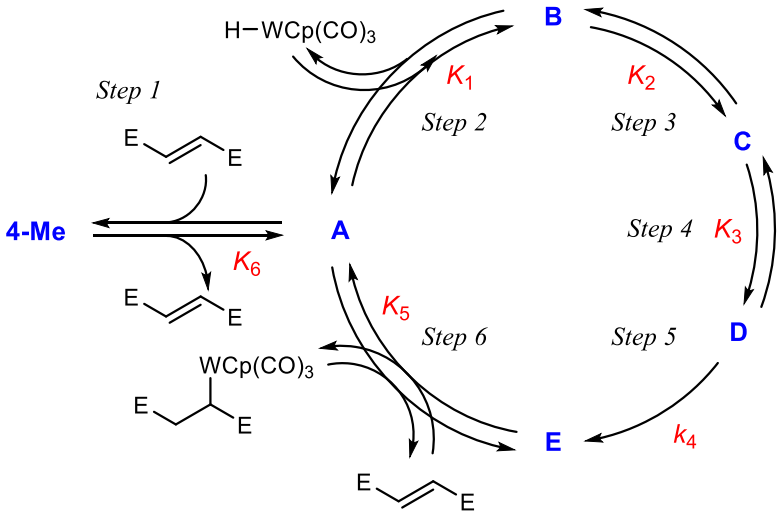

$$[\mathrm{Pd}]_{\mathrm{total}} = [\mathbf{A}] + [\mathbf{B}] + [\mathbf{C}] + [\mathbf{D}] + [\mathbf{E}] + [\mathbf{4\text{-}Me}] \quad \text{(Eq.S1)}$$

$$K_1 = \frac{[\mathbf{B}]}{[\mathbf{A}][\mathrm{WHCp(CO)_3}]} \quad \text{(Eq.S2)}$$

$$K_2 = \frac{[\mathbf{C}]}{[\mathbf{B}]} \quad \text{(Eq.S3)}$$

$$K_3 = \frac{[\mathbf{D}]}{[\mathbf{C}]} \quad \text{(Eq.S4)}$$

$$K_5 = \frac{[\mathbf{A}][\mathrm{Product}]}{[\mathbf{E}][\mathrm{Alkene}]} \quad \text{(Eq.S5)}$$

$$K_6 = \frac{[\mathbf{A}][\mathrm{Alkene}]}{[\mathbf{4-Me}]} \quad \text{(Eq.S6)}$$

From Eq.S6, we have Eq.S7

$$[\mathbf{4\text{-}Me}] = \frac{[\mathbf{A}][\mathrm{Alkene}]}{K_6} \quad \text{(Eq.S7)}$$

From Eq.S3, we have Eq.S8

$$[\mathbf{A}] = \frac{[\mathbf{B}]}{K_1[\mathrm{WHCp(CO)_3}]} \quad \text{(Eq.S8)}$$

From Eq.S2, we have Eq.S9

$$[\mathbf{B}] = \frac{[\mathbf{C}]}{K_2} \quad \text{(Eq.S9)}$$

From Eq.S3, we have Eq.S10

$$[\mathbf{C}] = \frac{[\mathbf{D}]}{K_3} \quad \text{(Eq.S10)}$$

From Eq.S5, we have Eq.S11

$$[\mathbf{E}] = \frac{[\mathbf{A}][\mathrm{Product}]}{K_5[\mathrm{Alkene}]} \quad \text{(Eq.S11)}$$

With substitution of [**C**] in Eq.S9 for Eq.S7, we have Eq.S12.

$$[\mathbf{B}] = \frac{[\mathbf{D}]}{K_2K_3} \quad \text{(Eq.S12)}$$

With substitution of [**B**] in Eq.S8 for Eq.S8, we have Eq.S13.

$$[\mathbf{A}] = \frac{[\mathbf{D}]}{K_1K_2K_3[\mathrm{WHCp(CO)_3}]} \quad \text{(Eq.S13)}$$

With substitution of [**A**] in Eq.S11 for Eq.S13, we have Eq.S14

$$[\mathbf{E}] = \frac{[\mathbf{D}][\mathrm{Product}]}{K_1K_2K_3K_5[\mathrm{Alkene}][\mathrm{WHCp(CO)_3}]} \quad \text{(Eq.S14)}$$

With substitution of [**A**] in Eq.S7 for Eq.S13, we have Eq.S15.

$$[\mathbf{4\text{-}Me}] = \frac{[\mathbf{D}][\mathrm{Alkene}]}{K_1K_2K_3K_6[\mathrm{WHCp(CO)_3}]} \quad \text{(Eq.S15)}$$

With Eqs S8,12-15, Eq. S1 is expressed as Eq. S16.

$$[\mathrm{Pd}]_{\mathrm{total}} = \frac{[\mathbf{D}]}{K_1K_2K_3[\mathrm{WHCp(CO)_3}]} + \frac{[\mathbf{D}]}{K_2K_3} + \frac{[\mathbf{D}]}{K_3} + [\mathbf{D}] + \frac{[\mathbf{D}][\mathrm{Product}]}{K_1K_2K_3K_5[\mathrm{Alkene}][\mathrm{WHCp(CO)_3}]} + \frac{[\mathbf{D}][\mathrm{Alkene}]}{K_1K_2K_3K_6[\mathrm{WHCp(CO)_3}]}$$

$$= \frac{K_5K_6[\mathrm{Alkene}] + K_1K_5K_6[\mathrm{WHCp(CO)_3}][\mathrm{Alkene}] + K_1K_2K_5K_6[\mathrm{WHCp(CO)_3}][\mathrm{Alkene}] + K_1K_2K_3K_5K_6[\mathrm{Alkene}][\mathrm{WHCp(CO)_3}] + K_6[\mathrm{Product}] + K_5[\mathrm{Alkene}]^2}{K_1K_2K_3K_5K_6[\mathrm{Alkene}][\mathrm{WHCp(CO)_3}]}[\mathbf{D}]$$

(Eq.S16)

From Eq.S16, we have Eq.S17

$$[\mathbf{D}]$$

$$= \frac{K_1K_2K_3K_5K_6[\mathrm{Alkene}][\mathrm{WHCp(CO)_3}][\mathrm{Pd}]_{\mathrm{total}}}{K_5K_6[\mathrm{Alkene}] + K_1K_5K_6[\mathrm{WHCp(CO)_3}][\mathrm{Alkene}] + K_1K_2K_5K_6[\mathrm{WHCp(CO)_3}][\mathrm{Alkene}] + K_1K_2K_3K_5K_6[\mathrm{Alkene}][\mathrm{WHCp(CO)_3}] + K_6[\mathrm{Product}] + K_5[\mathrm{Alkene}]^2}$$

(Eq.S17)

The formation rate of product can be expressed as shown in Eq. S16.

$$\frac{\mathrm{d}[\mathrm{Product}]}{\mathrm{dt}} = k_4[\mathbf{D}] \quad \text{(Eq.S18)}$$

With substitution of [**D**] in Eq. S17 for Eq. S18, we have Eq. S19.

$$\frac{\mathrm{d}[\mathrm{Product}]}{\mathrm{dt}}$$

$$= \frac{k_4K_1K_2K_3K_5K_6[\mathrm{Alkene}][\mathrm{WHCp(CO)_3}][\mathrm{Pd}]_{\mathrm{total}}}{K_5K_6[\mathrm{Alkene}] + K_1K_5K_6[\mathrm{WHCp(CO)_3}][\mathrm{Alkene}] + K_1K_2K_5K_6[\mathrm{WHCp(CO)_3}][\mathrm{Alkene}] + K_1K_2K_3K_5K_6[\mathrm{Alkene}][\mathrm{WHCp(CO)_3}] + K_6[\mathrm{Product}] + K_5[\mathrm{Alkene}]^2}$$

(Eq.S19)

Since **4-Me** is only observed as palladium spices during the catalytic reaction, we assume the equilibrium constant is $K_6 \ll 1$. Therefore at initial stage of catalytic reaction, K_6[Product] is assumed to be almost zero. Eq. S20 is reduced to Eq.S21

$$\frac{\mathrm{d}[\mathrm{Product}]}{\mathrm{dt}} = \frac{k_4K_1K_2K_3K_5K_6[\mathrm{Alkene}][\mathrm{WHCp(CO)_3}][\mathrm{Pd}]_{\mathrm{total}}}{K_5K_6[\mathrm{Alkene}] + K_1K_5K_6[\mathrm{WHCp(CO)_3}][\mathrm{Alkene}] + K_1K_2K_5K_6[\mathrm{WHCp(CO)_3}][\mathrm{Alkene}] + K_1K_2K_3K_5K_6[\mathrm{Alkene}][\mathrm{WHCp(CO)_3}] + K_5[\mathrm{Alkene}]^2}$$

$$\frac{\mathrm{d}[\mathrm{Product}]}{\mathrm{dt}} = \frac{k_4K_1K_2K_3[\mathrm{WHCp(CO)_3}][\mathrm{Pd}]_{\mathrm{total}}}{1 + K_1[\mathrm{WHCp(CO)_3}] + K_1K_2[\mathrm{WHCp(CO)_3}] + K_1K_2K_3[\mathrm{WHCp(CO)_3}] + [\mathrm{Alkene}]/K_6} \quad \text{(Eq.S20)}$$

$$\frac{\mathrm{d[Product]}}{\mathrm{dt}} = \frac{k_4 K_1 K_2 K_3 [\mathrm{WHCp(CO)_3}][\mathrm{Pd}]_{\mathrm{total}}}{1 + K_1[\mathrm{WHCp(CO)_3}](1 + K_1 + K_2 K_3) + [\mathrm{Alkene}]/K_6} \quad \text{(Eq.S21)}$$

Since the equilibrium constant is $K_6 \ll 1$, $[\mathrm{Alkene}]/K_6$ is much larger than 1 and $K_1[\mathrm{WHCp(CO)_3}](1 + K_2 + K_2 K_3)$. Eq. S21 is reduced to Eq. S22

$$\frac{\mathrm{d[Product]}}{\mathrm{dt}} = \frac{k_4 K_1 K_2 K_3 [\mathrm{WHCp(CO)_3}][\mathrm{Pd}]_{\mathrm{total}}}{[\mathrm{Alkene}]/K_6} = \frac{k_4 K_1 K_2 K_3 K_6 [\mathrm{WHCp(CO)_3}][\mathrm{Pd}]_{\mathrm{total}}}{[\mathrm{Alkene}]} \quad \text{(Eq.S22)}$$

3. DFT calculations

The density functional theory (DFT) calculations were employed with long-range and dispersion corrected ωB97X-D functional.[1] The basis set was consisted of the Stuttgart–Dresden SDD effective core potential basis set on the Pa and W atoms[2] and the 6-31G(d,p) basis sets on all other atoms.[3] Effect of benzene as a solvent was included in the calculations by using the Polarizable Continuum Model (PCM) using the integral equation formalism variant (IEFPCM).[4] The optimized molecular structures were verified by vibrational analysis; equilibrium structures did not have imaginary frequencies and transition state structures had only one imaginary frequency corresponding to the reaction coordinate. Additionally, the intrinsic reaction coordinate (IRC) calculations[5,6] were carried out to check whether the transition state leads to the reactant and the product, or not. Relative energies were corrected by adding the unscaled zero-point vibrational energy. All calculations were carried out using the Gaussian 09 program.[7]

Table S7. Calculated free energies.

Entry	Compounds	G /kcal mol^{-1}
1	$WHCp(CO)_3$	-377184.3622
2	dimethyl fumarate	-335134.1872
3	$W\{CH(CO_2Me)(CH_2CO_2Me)\}Cp(CO)_3$	-712325.5642
4	**4-Me**	-704701.6733
5	Pd(dimethyl fumarate)(PMe_3) (**A**)	-704701.6733
6	(Me_3P)(dimethyl fumarate)Pd(μ-H)(μ-CO)$WCp(CO)_3$ (**B**)	-1081898.439
7	**TS-1**	-1081886.181
8	*trans*-(Me_3P)\{($MeCO_2$)($MeCO_2CH_2$)CH\}Pd–$WCp(CO)_3$ (**C**)	-1081891.05
9	*cis*-(Me_3P)\{($MeCO_2$)($MeCO_2CH_2$)CH\}Pd–$WCp(CO)_3$ (**D**)	-1081894.724
10	**TS-2**	-1081880.813
11	$W\{CH(CO_2Me)(CH_2CO_2Me)\}Cp(CO)(\mu\text{-}CO)_2Pd(PMe_3)$ (**E**)	-1081896.384

Calculation of $K_{\mathbf{B\text{-}D}(H)}/K_{\mathbf{B\text{-}D}(D)}$ ratio

The equilibrium constants between intermediates **B** and **D** for the reaction with $WHCp(CO)_3$ or $WDCp(CO)_3$, $K_{\mathbf{B\text{-}D}(H)}$ and $K_{\mathbf{B\text{-}D}(D)}$ were estimated from free energy value as follows:

$K_{\mathbf{B\text{-}D}(H)} = \exp(-\Delta G_{\mathbf{B\text{-}D}}(H)/RT) = \exp\{-(3.7 \times 10^3 \text{ cal mol}^{-1})/(1.987 \text{ cal K}^{-1} \text{ mol}^{-1} \times 278.25 \text{ K})\} = 1.24 \times 10^{-3}$

$K_{\mathbf{B\text{-}D}(D)} = \exp(-\Delta G_{\mathbf{B\text{-}D}}(D)/RT) = \exp\{-(3.0 \times 10^3 \text{ cal mol}^{-1})/(1.987 \text{ cal K}^{-1} \text{ mol}^{-1} \times 278.25 \text{ K})\} = 4.40 \times 10^{-3}$

$K_{\mathbf{B\text{-}D}(H)}/K_{\mathbf{B\text{-}D}(D)}$ ratio was calculated as follows:

$K_{\mathbf{B\text{-}D}(H)}/K_{\mathbf{B\text{-}D}(D)} = (1.24 \times 10^{-3})/(4.40 \times 10^{-3}) = 0.281$

References

(1) Chai, J.-D.; Head-Gordon, M. *Phys. Chem. Chem. Phys.* **2008**, *10*, 6615-6620.

(2) (a) Szentpaly, L. V.; Fuentealba, P.; Preuss, H.; Stoll, H. *Chem. Phys. Lett.* **1982**, *93*, 555-559. (b) Dolg, M.; Wedig, U.; Stoll, H.; Preuss H. *J. Chem. Phys.* **1987**, *86*, 866-872. (c) Schwerdtfeger, P.; Dolg, M.; Schwarz, W. H. E.; Bowmaker, G.A.; Boyd P. D. W. *J. Chem. Phys.* **1989**, *91*, 1762-1774.

(3) Hehre, W. J.; Radom, L.; Schleyer, P. V. R.; Pople, J. A. In *Ab Initio Molecular Orbital Theory*; Wiley: New York, 1986.

(4) As a review for PCM models, see: Tomasi, J.; Mennucci, B.; Cammi R. *Chem. Rev.* **2005**, *105*, 2999-3093.

(5) Fukui, K. *J. Phys. Chem.* **1970**, *74*, 4161-4163.

(6) Hratchian, H. P.; Schlegel H.B. *J. Chem. Theory Comput.* **2005**, *1*, 61-69.

(7) Frisch, M. J.; Trucks, G. W.; Schlegel, H. B.; Scuseria, G. E. ; Robb, M. A.; Cheeseman, J. R.; Scalmani, G. ; Barone, V.; Mennucci, B.; Petersson, G. A. ; Nakatsuji, H. ; Caricato, M.; Li, X.; Hratchian, H. P.; Izmaylov, A. F.; Bloino, J. ; Zheng, G. : Sonnenberg, J. L. ; Hada, M.; Ehara, M.; Toyota, K.; Fukuda, R.; Hasegawa, J.; Ishida, M.; Nakajima, T.; Honda, Y.; Kitao, O.; Nakai, H.; Vreven, T.; Montgomery, Jr. J. A.; Peralta, J. E.; Ogliaro, F.; Bearpark, M. ; Heyd, J. J.; Brothers, E.; Kudin, K. N.; Staroverov, V.N.; Kobayashi, R.; Normand, J.; Raghavachari, K.; Rendell, A.; Burant, J. C.; Iyengar, S. S.; Tomasi, J.; Cossi, M.; Rega, N.; Millam, J. M.; Klene, M.; Knox, J. E.; Cross, J. B.; Bakken, V.; Adamo, C.; Jaramillo, J.; Gomperts, R.; Stratmann, R. E.; Yazyev, O. ; Austin, A. J.; Cammi, R.; Pomelli, C.; Ochterski, J. W.; Martin, R. L.; Morokuma, K.; Zakrzewski, V. G.; Voth, G. A.; Salvador, P.; Dannenberg, J. J.; Dapprich, S.; Daniels, A. D.; Farkas, Ö.; Foresman, J. B.; Ortiz, J. V.; Cioslowski, J.; Fox, D. J. *Gaussian 09, Revision C.01*, Gaussian, Inc., Wallingford CT (2009).